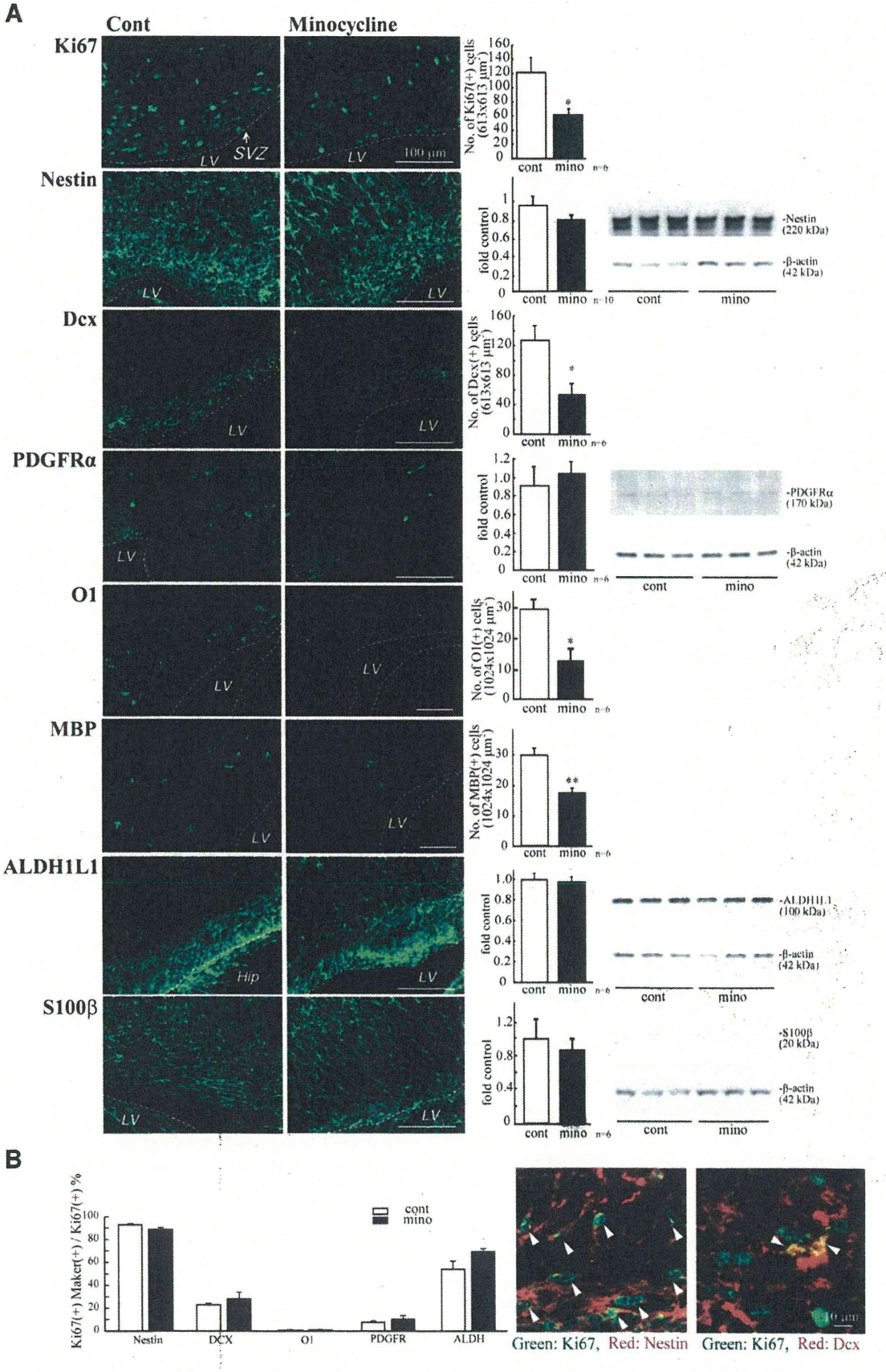

Figure 4. Minocycline decreased the numbers of proliferating cells, neuronal progenitors, and oligodendrocyte progenitors in the early postnatal SVZ. ***A***, Minocycline was administered by intraperitoneal injection for 3 d beginning at P2 (30 mg/kg/d, P2-P4, $n = 6$/group). Sagittal sections of forebrains were immunostained with antibodies to Ki67, nestin, Dcx, PDGFRα, O1, MBP, ALDH1L1, and S100β. The numbers of cells positive for Ki67, Dcx, MBP, or O1 were counted, whereas the protein levels of nestin, PDGFRα, ALDH1L1, and S100β (*Figure legend continues.*)

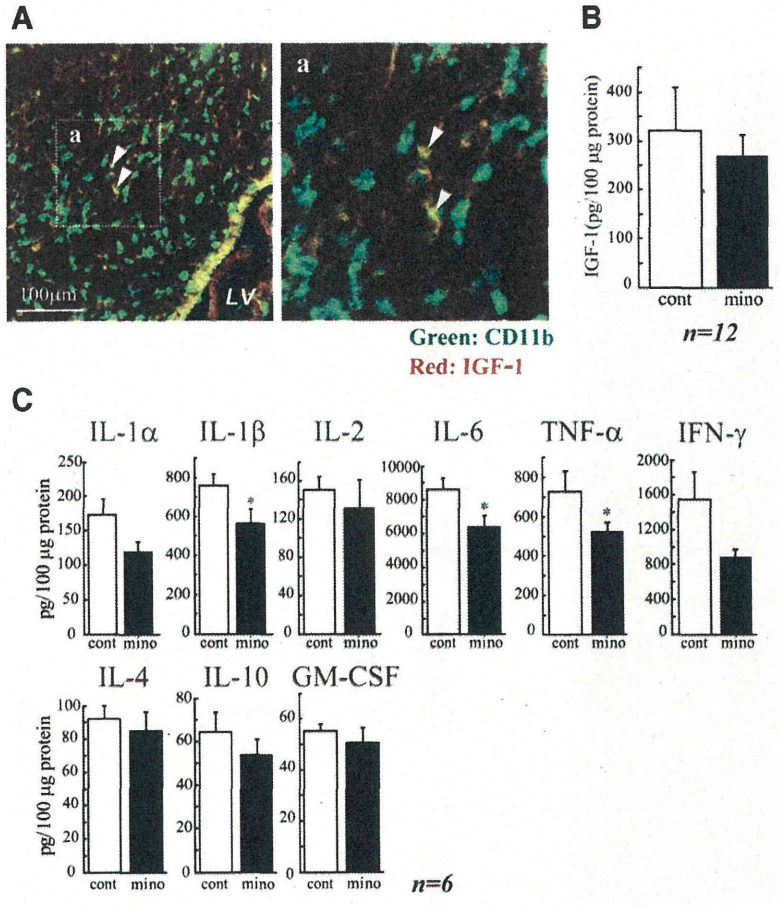

Figure 5. The activated microglia raised the cytokine levels in the SVZ. ***A***, A subpopulation of the microglia express IGF-1 in the early postnatal SVZ, but IGF-1 is not involved in the action of activated microglia during this period. Sagittal sections were immunostained with anti-CD11b (green: microglia) and anti IGF-1 (red) antibodies. Right panel, Magnified image of the square in the left. A subpopulation of microglia is positive for IGF-1 (arrowheads). The percentage of CD11b$^+$IGF-1$^+$ was 43.42 ± 6.72% in CD11b$^+$ cells. ***B***, Minocycline did not affect the amount of IGF-1 in the early postnatal SVZ. Minocycline was administered by intraperitoneal injection for 3 d beginning at P2 (30 mg/kg/d, P2-P4, n = 6/group), and the amount of IGF-1 in the SVZ was quantified by ELISA. ***C***, Minocycline decreased the amount of inflammatory cytokines in the SVZ. IL-1α, IL-1β, IL-2, IL-4, IL-6, IL-10, GM-CSF, IFN-γ, and TNF-α levels in the SVZ tissue lysate were measured by BioPlex cytokine detection assay system. *$p <$ 0.05 (Student's t test). n = 6 rats/group. Data are mean ± SEM. Similar results were obtained in two independent experiments.

remarkably decreased at P30. These results are consistent with those obtained from the sagittal sections (Fig. 1), showing the population of activated microglia that accumulated within the SVZ during the early postnatal period.

We therefore examined the specific roles of these microglia in the early postnatal SVZ. At early postnatal ages, both neurogenesis and gliogenesis are active in the SVZ (Gould et al., 1999; Wagner et al., 1999; Doetsch and Scharff, 2001; Zerlin et al., 2004; Marshall et al., 2008). To suppress the activation of microglia, we used minocycline, a tetracycline antibiotic, long used to suppress microglial activation (Tikka et al., 2001; Zhao et al., 2007). We first verified the effects of minocycline on the activation of microglia. Minocycline was administered by intraperitoneal injection for 3 d beginning at P2 (30 mg/kg/d, P2-P4, n = 6/group), and sagittal sections of minocycline-treated rat forebrains were immunostained for Iba1, CD11b, and CD68. Minocycline did not change the numbers of Iba1-positive microglia in the VZ/SVZ (Fig. 3*A*, top), but it dramatically changed their shape from amoeboid to more ramified (Fig. 3*A*, bottom). The number of CD11b$^+$ cells was significantly decreased (Fig. 3*Bb1*, top and graph), and the decrease in CD11b levels in the SVZ was confirmed by Western blotting (Fig. 3*Bb2*, top graph and photo). The number of CD68$^+$ cells and the level of CD68 were also decreased (Fig. 3*B*, bottom data). These results indicate that our administration of minocycline suppresses the activation of SVZ microglia.

We then investigated the effects of minocycline on early postnatal differentiation. After the administration of minocycline, sagittal sections were immunostained with differentiation markers: Ki67 (proliferating cells), nestin (stem cells), Dcx (neuronal progenitors), PDGFRα (oligodendrocyte progenitors [polydendrocytes]), O1 (oligodendrocyte progenitors [premyelinating oligodendrocytes]), MBP (mature oligodendrocyte [premyelinating and myelinating oligodendrocytes] (Nishiyama et al., 2009), ALDH1L1 (astrocyte progenitors), and S100β$^+$ (astrocytes) (Fig. 4*A*). The numbers of cells positive for Ki67, Dcx, O1, and MBP were counted, whereas the levels of nestin, PDGFα, ALDH1L1, and S100β were examined by Western blotting because it was hard to discriminate the cell morphologies by these signals. Minocycline significantly decreased the number of Ki67$^+$ cells and slightly decreased the level of nestin. The number of cells positive for Dcx was also significantly reduced. Furthermore, minocycline decreased the numbers of cells positive for O1 and MBP, whereas the numbers of PDGFRα$^+$ cells rather tended to increase. The levels of ALDH1L1 and S100β did not change. These results suggest that activated microglia in the early postnatal SVZ enhance neurogenesis and oligodendrogenesis, and activated microglia affect oligodendrocyte progenitors at rather later stage of differentiation. We also performed the double staining of Ki67 with the respective differentiation markers (Fig. 4*B*). Although the total number of Ki67$^+$ cells was decreased by minocycline, consistent with Figure 4*A*, the percentage of Ki67$^+$ cells also positive for the respective differentiation markers did not change in the absence or presence of minocycline (Fig. 4*B*, left graph), suggesting that minocycline did not affect the proliferation of progenitors of the specific cell types. Typical images of the SVZ cells positive for

(*Figure legend continued.*) were examined by Western blotting. Minocycline significantly decreased the number of Ki67$^+$ proliferating cells and decreased the level of nestin. The number of cells positive for Dcx was significantly reduced. Minocycline decreased the numbers of cells positive for O1 and MBP, whereas the expression level of PDGFRα tended to increase. *$p <$ 0.05, **$p < 0.01$ (Student's t test). n = 6 mice/group. Data are mean ± SEM. ***B***, The ratio of the Ki67$^+$ cells also positive for respective differentiation markers did not change in the absence or presence of minocycline (left graph). Typical images of the cells positive for Ki67 and Nestin, and the cells positive for Ki67 and Dcx in the control group are shown (right panels). We confirmed the same results in three independent experiments.

Ki67 and Nestin, and the cells positive for Ki67 and Dcx in the control group are shown (Fig. 4*B*, right panels).

Butovsky et al. (2006a) have reported that IGF-1 released from activated microglia promoted neurogenesis and oligodendrogenesis from adult stem/progenitor cells. We examined whether microglia in the early postnatal SVZ produce IGF-1 (Fig. 5*A*). Microglia did contain IGF-1 protein, but the percentage of $CD11b^+$ cells also positive for $IGF\text{-}1^+$ was 43.42 ± 6.72%. Furthermore, the amount of IGF-1 in the SVZ tissue lysates was not decreased by minocycline (Fig. 5*B*). These results suggest that, although a fraction of activated microglia in the early postnatal SVZ did produce IGF-1, the effects of activated microglia on neurogenesis and oligodendrogenesis obtained in our study were independent of IGF-1. Activated microglia release a number of cytokines. In some cases other than pathological conditions, cytokines also have physiological roles (Schäfers and Sorkin, 2008; Spedding and Gressens, 2008; Camacho-Arroyo et al., 2009; Miller et al., 2009; Spooren et al., 2011). We therefore investigated whether the SVZ microglia cause the increase in cytokine concentrations in the early postnatal SVZ (Fig. 5*C*). We examined the effects of minocycline on the levels of IL-1α, IL-1β, IL-2, IL-4, IL-6, IL-10, GM-CSF, IFN-γ, and TNF-α. To measure multiple cytokines in a small volume of tissue samples simultaneously, we used the BioPlex cytokine detection assay system (Bio-Rad). The levels of IL-1β, IL-6, and TNF-α were significantly decreased by the 3-day intraperitoneal administration of minocycline (Fig. 5*C*). Although the difference was not significant, the level of IFN-γ also tended to be decreased.

To examine more directly whether these cytokines affected neurogenesis and oligodendrogenesis, we performed *in vitro* experiments, coculturing neural stem cells with activated microglia. Microglia cultured independently of neurospheres on transwells were activated by LPS (10 ng/ml, 30 min) in the presence or absence of minocycline (10 μM). The microglia were carefully washed to remove residual LPS and minocycline, and then the transwell on which microglia were cultured was set onto the neurosphere cultures in prodifferentiation conditions. The activated microglia significantly increased the number of $\beta3\text{-tubulin}^+$ and $O4^+$ cells but had no effects on $GFAP^+$ cells in neurospheres (Fig. 6*A*,*B*). Minocycline almost completely suppressed the effects of activated microglia on the numbers of cells positive

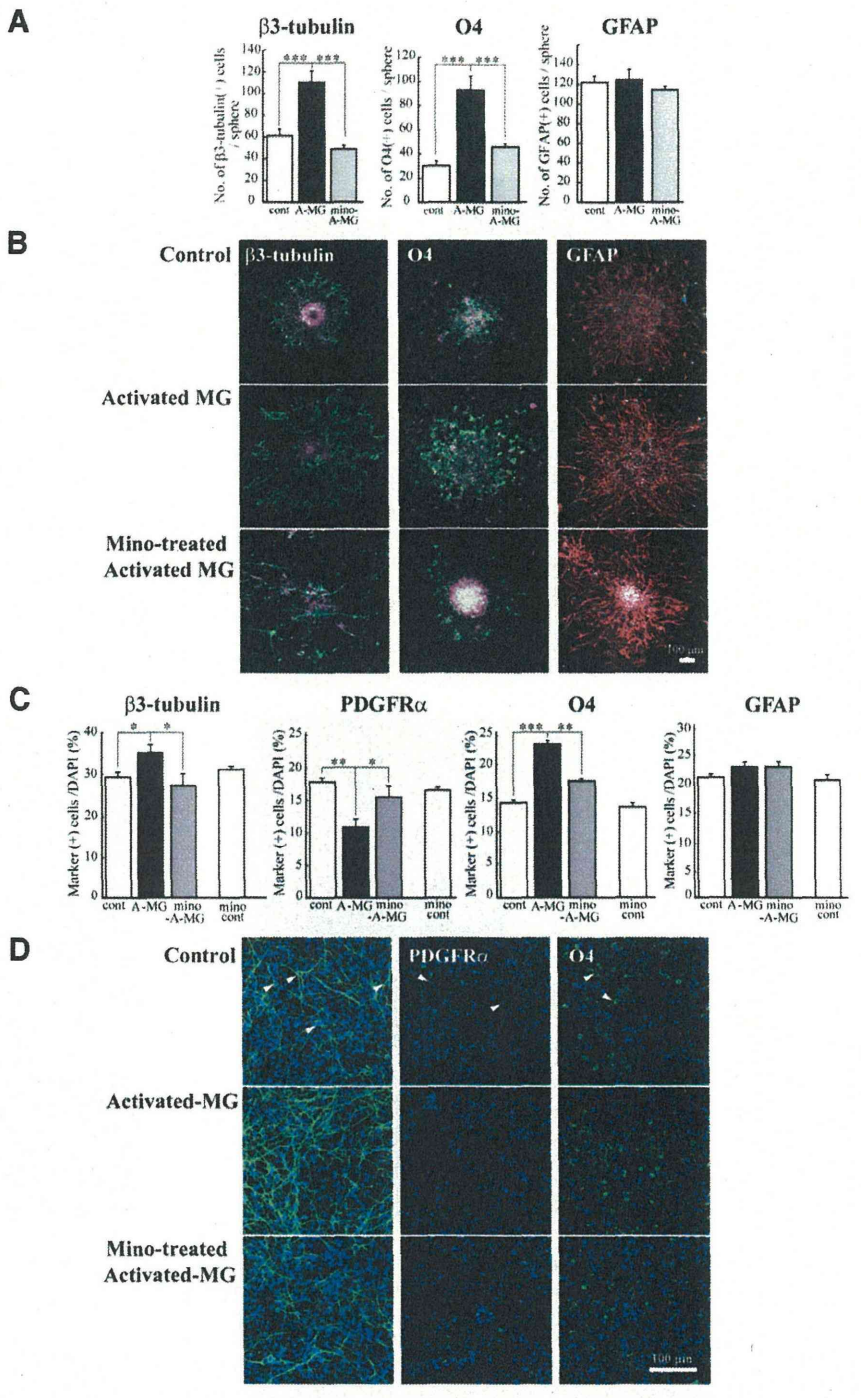

Figure 6. The reproduction of the enhancement of neurogenesis and oligodendrogenesis by activated microglia *in vitro*. Microglia cultured independently of neurosphere on transwells were activated by LPS (10 ng/ml, 30 min) in the presence or absence of minocycline (10 μM), washed carefully, and the transwells were set onto the neurospheres or dissociated cells from neurosphere in prodifferentiation conditions. After differentiation periods suitable for neurons (7 d) or oligodendrocytes (11 d), neurospheres were stained for β3-tubulin (green), PDGFRα (green), O4 (green), GFAP (red), and TOTO3 (cyan). To check the effects of minocycline alone, dissociated cells were incubated in the presence of minocycline (10 μM) for 7 d. ***A***, Quantification of the numbers of neurons, oligodendrocyte progenitors, or astrocytes differentiated from neurospheres cocultured with activated microglia in the presence or absence of minocycline. $^{***}p < 0.001$ (Tukey's test by ANOVA). $n = 12$ neurospheres/group. Data are mean ± SEM. ***B***, Representative immunostained images of neurospheres cocultured with activated microglia in the presence or absence of minocycline. ***C***, The effects of activated microglia on differentiation of single cells dissociated from neurospheres in the presence or absence of minocycline. The effects of minocycline alone were also shown (mino-cont in each graph). $^{*}p < 0.05$, $^{**}p < 0.01$, $^{***}p < 0.001$. (Tukey's test by ANOVA). $n = 12$ neurospheres/group. Data are mean ± SEM. ***D***, Images of cells immunostained for differentiation markers. Arrowheads indicate the representative cells positive for the differentiation markers.

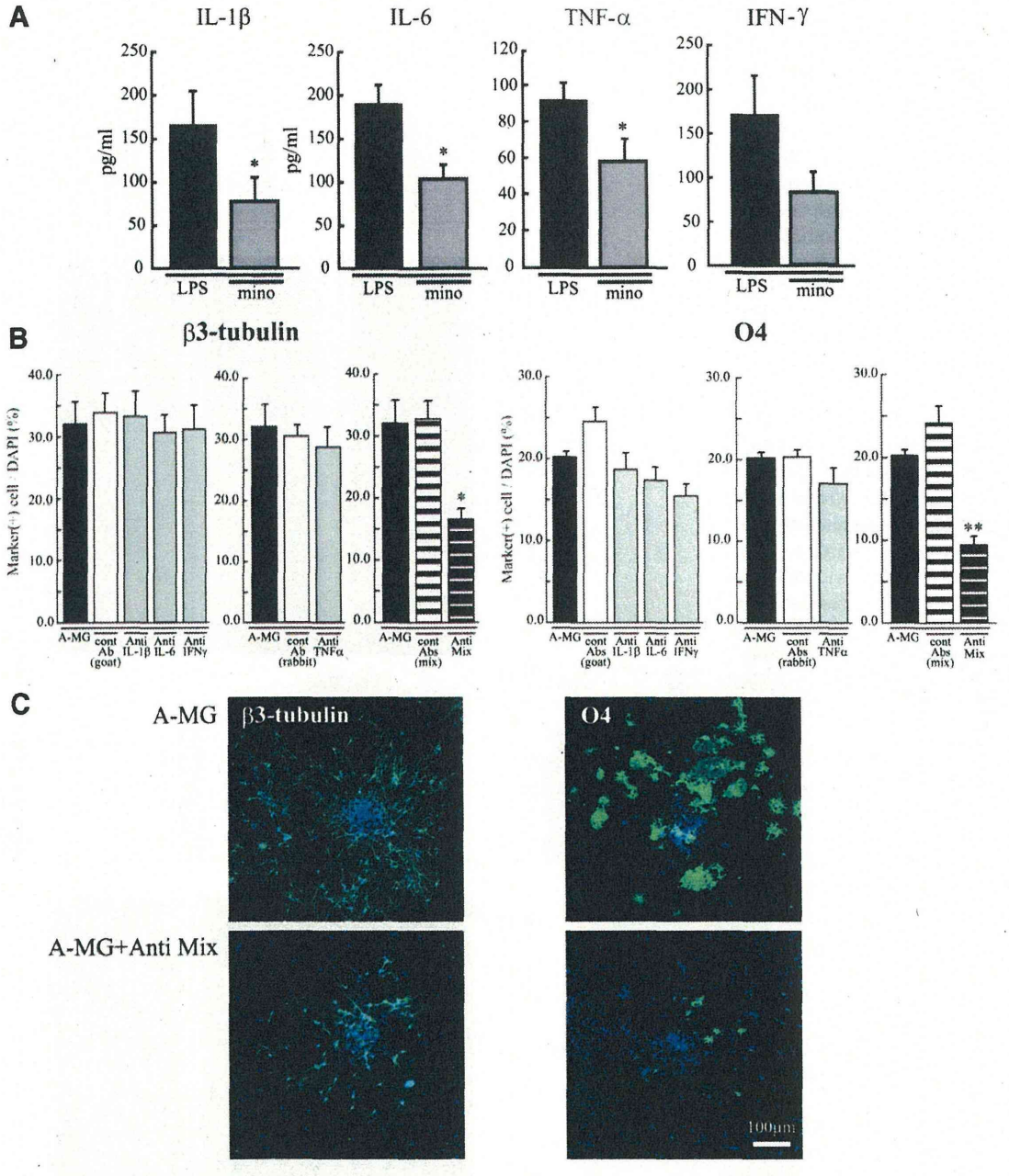

Figure 7. The *in vitro* enhancement of neurogenesis and oligodendrogenesis by activated microglia was suppressed by the mixture of function-blocking antibodies (anti-IL-1β, anti-IL-6, anti-TNF-α, and anti-IFN-γ). ***A***, The release of IL-1β, IL-6, TNF-α, or IFN-γ from activated microglia was suppressed by minocycline. Cultured microglia were activated by LPS (10 ng/ml, 30 min) in the absence and presence of minocycline (10 μM). The concentration of each cytokine in the supernatant was measured by ELISA 24 h after. *$p < 0.05$ (Student's *t* test). Data are mean ± SEM. ***B***, Effects of function-blocking antibodies to IL-1β, IL-6, TNF-α, and IFN-γ on enhanced neurogenesis and oligodendrogenesis by the activated microglia. The neurospheres were differentiated in the absence or presence of functional blocking antibodies (goat anti-rat IL-1β antibody, goat anti-rat IL-6 antibody, TNF-α antibody, or goat anti-mouse/rat IFN-γ antibody) (1 μg/ml for each) and a mixture of all of these antibodies. After a differentiation period suitable for neurons (7 d) or oligodendrocytes (11 d), neurospheres were stained for β3-tubulin (green), O4 (green), and TOTO3 (cyan). The data of single function blocking antibodies were compared with the controls, which include the same concentration of isotype-matched control IgGs (1 μg/ml for each). The data of the mixture of function blocking antibodies were compared with the controls, which include the same concentrations of isotype-matched control IgGs (i.e., 3 μg/ml of normal goat IgG control and 1 μg/ml of rabbit IgG control). *$p < 0.05$. **$p < 0.01$, versus isotype-matched control IgG group (Tukey's test by ANOVA). Data are mean ± SEM. ***C***, Representative immunostained images of neurospheres cocultured with activated microglia in the absence or presence of the mixture of the function-blocking antibodies. We confirmed the same results in three independent experiments.

for β3-tubulin or O4. We further confirmed these results using a differentiation assay with cells dissociated from neurospheres (Fig. 6*C*,*D*). With this protocol, the morphology of each cell could be discriminated more clearly. Consistent with the results described above, an increase in the numbers of cells positive for β3-tubulin and O4 was induced by activated microglia (Fig. 6*C*,*D*). Of note, PDGFRα$^+$ cells were decreased by activated microglia, whereas O4$^+$ cells were increased by activated microglia. Minocycline suppressed both of these effects, suggesting that activated microglia affect the later stage of oligodendrogenesis, thereby reducing the size of PDGFα$^+$ progenitor pool. In this experiment, we also checked the effects of minocycline alone (10 μM) on neurogenesis and oligodendrogenesis (Fig. 6*C*, "mino-cont" in each graph). Minocycline did not affect the numbers of

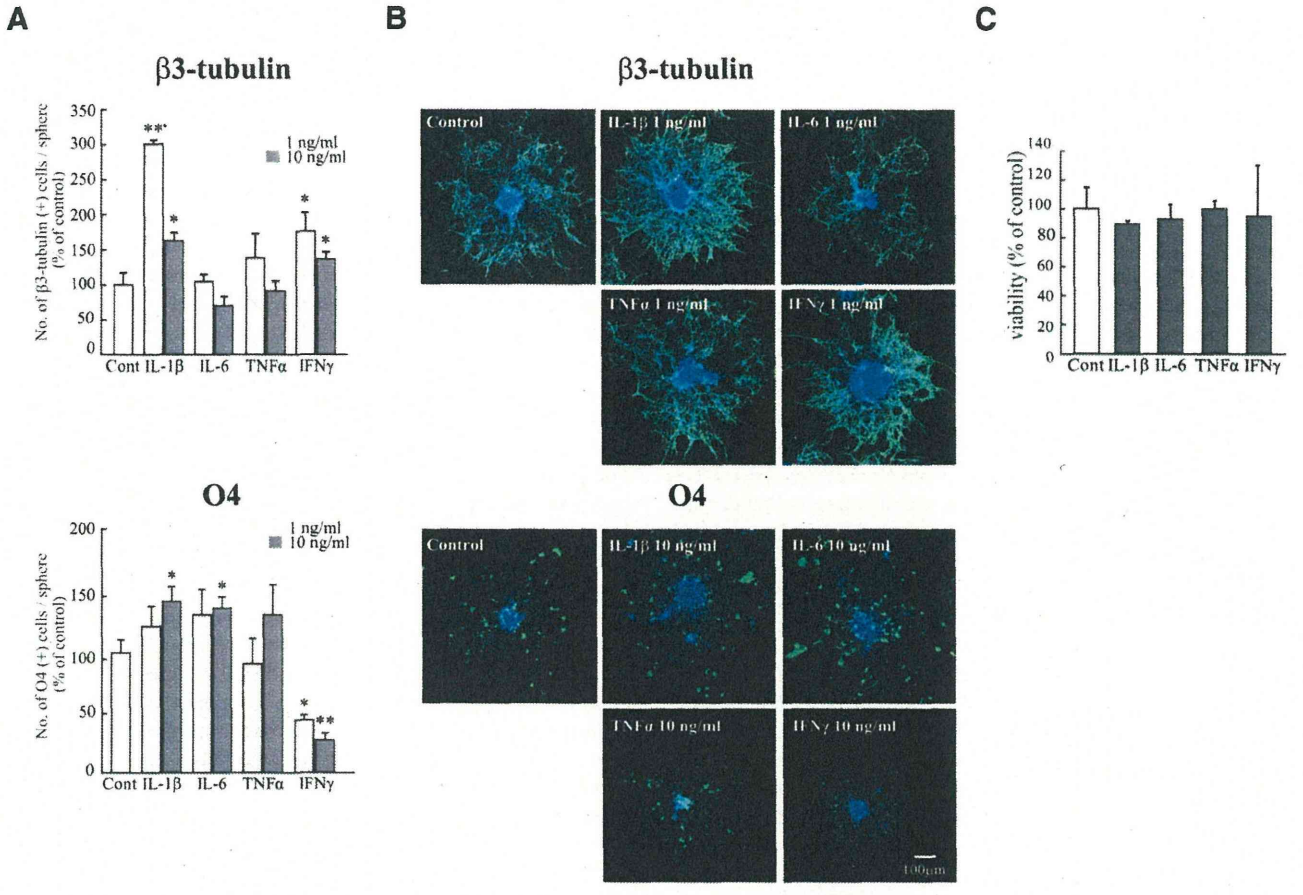

Figure 8. The effect of each cytokine on neurogenesis and oligodendrogenesis. Neurospheres were incubated for differentiation period suitable for neurons (7 d) or oligodendrocytes (11 d) in the presence of each single cytokine (rIL-1β, rIL-6, rTNF-α, or rIFN-γ) at 1–10 ng/ml. Neurospheres were stained for β3-tubulin (green), O4 (green), followed by TOTO3 (cyan). ***A***, Quantification of the effects of cytokines on neurogenesis and oligodendrogenesis. IL-1β and IFN-γ significantly enhanced neurogenesis at 1 ng/ml. IL-1β and IL-6 enhanced oligodendrogenesis at 10 ng/ml. $*p < 0.05$ versus control (Tukey's test by ANOVA). $**p < 0.01$ versus control (Tukey's test by ANOVA). $n = 8$ neurospheres/group. Data are mean ± SEM. ***B***, Representative images of neurospheres immunostained for β3-tubulin and O4 after differentiation in the presence of the cytokine. ***C***, The effect of each cytokine (10 ng/ml) on cell viability. They did not affect cell viability at 10 ng/ml. The same results were obtained in two independent experiments.

cells positive for β3-tubulin, O4, PDGFRα, or GFAP, indicating that minocycline itself had little direct effects on neurogenesis and oligodendrogenesis. Together, these results demonstrated that we could reproduce the *in vivo* data in an *in vitro* coculture experiment. We further confirmed that activated microglia enhanced neurogenesis and oligodendrogenesis, and minocycline specifically suppressed the effects of microglia. We therefore examined the effects of minocycline on the release of IL-1β, IL-6, TNF-α, and IFN-γ from activated microglia *in vitro*. In the presence of minocycline, the release of all of these cytokines was significantly suppressed (Fig. 7*A*), consistent with *in vivo* data (Fig. 5*C*). To examine the extent of the contribution of each cytokine to the enhancement of neurogenesis and oligodendrogenesis, we applied function-blocking antibodies to IL-1β, IL-6, TNF-α, and IFN-γ (1 μg/ml) to cocultures of activated microglia and neurospheres (Fig. 7*B*). The same concentration of isotype-matched control IgG (both of goat and rabbit) (1 μg/ml) did not have any effects on either neurogenesis or oligodendrogenesis. Unexpectedly, any single function-blocking antibody to IL-1β, IL-6, TNF-α, or IFN-γ did not change the effects of activated microglia on neurogenesis and oligodendrogenesis (Fig. 7*B*). We then tried a mixture of all of these function-blocking antibodies (goat anti-rat IL-1β antibody, goat anti-rat IL-6 antibody, TNF-α antibody, and goat anti-mouse/rat IFN-γ antibody, 1 μg/ml for each). When compared with the control which included the same concentrations of isotype-matched control IgGs (i.e., 3 μg/ml of normal goat IgG control and 1 μg/ml of rabbit IgG control), the effects of activated microglia were significantly suppressed by a mixture of all of these function-blocking antibodies (Fig. 7*B*, Anti Mix in the right graphs in β3-tubulin and O4, respectively). The representative images of the expression of β3-tubulin (left) or O4 (right) in neurospheres cocultured with activated microglia in the presence of the mixture of function-blocking antibodies are shown in Figure 7*C*. We also examined the direct effects of each single cytokine on neurogenesis and oligodendrogenesis separately (Fig. 8). IL-1β and IFN-γ enhanced neurogenesis at 1 ng/ml, although the effects became weaker at 10 ng/ml (Fig. 8*A*). IL-1β and IL-6 enhanced oligodendrogenesis at 10 ng/ml (Fig. 8*A*). IFN-γ suppressed oligodendrogenesis. These results suggest that IL-1β and IFN-γ are important for neurogenesis, whereas IL-1β and IL-6 are important for oligodendrogenesis, and the combinations and concentrations optimal for neurogenesis and oligodendrogenesis are different. Representative data of the neurospheres treated with the cytokines are shown in Figure 8*B*. We confirmed that each single cytokine did not affect cell viability at 10 ng/ml in our experimental protocol (Fig. 8*C*). These *in vitro* data indicate that activated microglia regulate neurogenesis and oligodendrogenesis through released cytokines, and the cyto-

kines produce their effects in a synergistic manner. It also appears that the combinations and concentrations optimal for neurogenesis and oligodendrogenesis are different.

Discussion

In the postnatal mammalian brain, neural stem cells (NSCs) are mainly localized in two areas: the forebrain SVZ (Doetsch and Scharff, 2001) and the subgranular zone of the dentate gyrus (Zerlin et al., 2004) of the hippocampus (Gould et al., 1999; Lie et al., 2004). The microenvironments that are permissive for neurogenesis and gliogenesis are composed of a variety of cell types, such as stem cells, progenitor cells, astrocyte cells, and microglial cells. Increasing evidence indicates the importance of the surrounding glial cells in neurogenesis (Doetsch et al., 1999; Temple, 2001). Goings et al. (2006) have shown that microglia in the adult SVZ are semiactivated, but microglial contribution to neurogenesis is complex. So far, the role of microglia in neurogenesis has been examined mainly in pathological conditions (Ekdahl et al., 2003; Monje et al., 2003). Activated microglia in inflammatory settings, such as intraperitoneal administration of LPS, inhibited neurogenesis (Ekdahl et al., 2003; Monje et al., 2003; Cacci et al., 2008). However, a growing number of studies have suggested that activated microglia are beneficial for neurogenesis (Aarum et al., 2003; Butovsky et al., 2005, 2006a; Walton et al., 2006; Ziv et al., 2006; Hanisch and Kettenmann, 2007; Ekdahl et al., 2009; Bachstetter et al., 2011; Ekdahl, 2012; Vukovic et al., 2012), even in pathological conditions, such as an animal model of multiple sclerosis (Butovsky et al., 2006b), ischemia (Thored et al., 2009; Deierborg et al., 2010), and epilepsy (Bonde et al., 2006). Such variability concerning the effects of microglia on neurogenesis may reflect the different polarization of microglia and/or the precise status of NSCs/neuronal progenitor cells (NPCs) (Cacci et al., 2008; Li et al., 2010; Ekdahl, 2012; Ortega et al., 2013), and crosstalk between them (Mosher et al., 2012).

Concerning the origin of microglia, various data have been reported. *In vivo* lineage tracing studies have established that microglia differentiate from primitive myeloid progenitors that arise before embryonic day 8 and are identified in the CNS parenchyma even before definitive hematopoiesis (Ginhoux et al., 2010), although it has been shown that microglia migrate from lateral ventricle into brain via SVZ in the postnatal brain (Mohri et al., 2003). Microglia in the embryonic SVZ limit the production of cortical neurons by phagocytosing neural precursor cells (Cunningham et al., 2013). Even in the adult brain, microglia appear densely populated in neurogenic niches, such as the SVZ (Mosher et al., 2012), and appear more activated in the adult SVZ than in non-neurogenic zones (Goings et al., 2006). Although these data strongly suggest that microglia play important roles in CNS development and an increasing number of studies have elucidated various roles of microglia during developmental periods (Wu et al., 1993; Pont-Lezica et al., 2011; Tremblay et al., 2011), the detailed dynamics of microglia in the SVZ from early postnatal stages to a young adult stage remain to be elucidated. Furthermore, few studies have examined the role of microglia in normal developmental processes during this period. In this study, we found that activated microglia first accumulated in the SVZ and then dispersed to white matter, where they became more ramified. In addition, the number of activated microglia was largest in the medial SVZ throughout the studied period (P30). We here elucidated that activated microglia in the early postnatal SVZ enhance neurogenesis and oligodendrogenesis through the mechanisms described below. Our present data and the previous reports concerning developmental changes in the distribution suggest that the developmental roles of microglia in the SVZ are not transient but more general throughout life.

Using a combination of *in vivo* and *in vitro* approaches, we demonstrated that these activated microglia in the early postnatal SVZ enhanced neurogenesis and oligodendrogenesis through releasing cytokines. Butovsky et al. (2006a) reported that the beneficial effects of microglia on adult neurogenesis/oligodendrogenesis was achieved by IGF-1 after IL-4 and IFN-γ release from activated microglia. In our study, although the activated microglia in the early postnatal SVZ did produce IGF-1, the effects of activated microglia on neurogenesis and oligodendrogenesis observed here were independent of IGF-1. We clarified that the SVZ microglia facilitate neurogenesis and oligodendrogenesis via production of cytokines. Interestingly, in *in vitro* coculture experiments, the enhancement of neurogenesis and oligodendrogenesis was suppressed by a mixture of function-blocking antibodies (anti-IL-1β, anti-IL-6, anti-TNF-α, anti-IFN-γ), but not by a single function-blocking antibody. These results suggest that microglial cytokines enhance neurogenesis and oligodendrogenesis in combinations. In support of this, among the cytokines we examined, only IL-1β and IFN-γ enhanced neurogenesis, whereas only IL-1β and IL-6 showed potentials of enhancing oligodendrogenesis. Previous reports have shown that NPCs express IL-1β, IL-1RI and IL-1RII, and IL-1β regulates the proliferation and differentiation of NPCs (Wang et al., 2007). It has been shown that IL-1β promotes proliferation and differentiation of oligodendrocyte progenitor cells (Vela et al., 2002). Furthermore, IL-6 and IL-6R are reported to promote neurogenesis and gliogenesis (Islam et al., 2009; Oh et al., 2010). Li et al. (2010) showed that IFN-γ stimulated neurosphere formation from embryonic brain, but the effects of IFN-γ are modified in the presence of microglia, supporting the complementary interactions between cytokines.

These proinflammatory cytokines had been thought to cause suppression of neurogenesis in pathological conditions, such as chronic LPS stimulation (Monje et al., 2003), allergic encephalomyelitis (Ben-Hur et al., 2003), and status epilepticus (Iosif et al., 2006; Koo and Duman, 2008). However, recent reports have shown that that the different polarizations of microglia are induced by different application protocols of LPS (Cacci et al., 2008), suggesting that the combination and the concentration of cytokines released by microglia change depending on the ambient conditions. Indeed, some previous reports suggest that each cytokine reveals different effects at different concentrations (Bernardino et al., 2008; Cacci et al., 2008; Das and Basu, 2008; Russo et al., 2011). Bernardino et al. (2008) have shown that TNF-α results in proliferation of neural stem cells at 1 ng/ml but caused apoptosis at 10–100 ng/ml. Microglia in the developmental brains may sense the change of environment and release a certain combination of cytokines at suitable concentrations for neurogenesis and oligodendrogenesis, whereas overactivation of microglia in pathological inflammation or nerve injury induces massive proinflammatory cytokine production, resulting in the suppression of neurogenesis. Nakanishi et al. (2007) showed that IL-6 promoted astrocytogenesis from the SVZ neurospheres. In our study, however, although activated microglia release IL-6, the effects on astrocytogenesis were not observed either *in vivo* or *in vitro*. This might be because of different medium compositions (i.e., growth factors) used for differentiation of neurosphere. Compared with the other cytokines, only IFN-γ suppressed oligodendrogenesis, suggesting that a proper concentration range of IFN-γ to enhance oligodendrogenesis might be narrower than the other cytokines.

Of interest, our results suggest that activated microglia significantly increased $O4^+$ cells while decreasing $PDGFR\alpha^+$ cells. These results suggest that activated microglia enhance oligodendrogenesis at later stages of oligodendrocyte differentiation. Recently, Miron et al. (2013) showed that a switch from M1 to M2 occurred in microglia during remyelination, and oligodendrocyte differentiation was enhanced by M2 cell releasing factors. A comprehensive analysis about the released factors from microglia, including cytokines, and the precise identification of the cell population (NSCs and/or NPCs) that are responsive to these factors will be necessary to understand fully the mechanisms underlying the effects of microglia on neurogenesis and gliogenesis.

In conclusion, we have found a population of activated microglia accumulating in the early postnatal SVZ that facilitate neurogenesis and oligodendrogenesis. A synergism among cytokines was important for the effects. To our knowledge, this is the first report to show that microglia regulate cell differentiation via releasing cytokines in early postnatal brain development.

References

Aarum J, Sandberg K, Haeberlein SL, Persson MA (2003) Migration and differentiation of neural precursor cells can be directed by microglia. Proc Natl Acad Sci U S A 100:15983–15988. CrossRef Medline

Bachstetter AD, Morganti JM, Jernberg J, Schlunk A, Mitchell SH, Brewster KW, Hudson CE, Cole MJ, Harrison JK, Bickford PC, Gemma C (2011) Fractalkine and CX 3 CR1 regulate hippocampal neurogenesis in adult and aged rats. Neurobiol Aging 32:2030–2044. CrossRef Medline

Ben-Hur T, Ben-Menachem O, Furer V, Einstein O, Mizrachi-Kol R, Grigoriadis N (2003) Effects of proinflammatory cytokines on the growth, fate, and motility of multipotential neural precursor cells. Mol Cell Neurosci 24:623–631. CrossRef Medline

Bernardino L, Agasse F, Silva B, Ferreira R, Grade S, Malva JO (2008) Tumor necrosis factor-alpha modulates survival, proliferation, and neuronal differentiation in neonatal subventricular zone cell cultures. Stem Cells 26:2361–2371. CrossRef Medline

Bonde S, Ekdahl CT, Lindvall O (2006) Long-term neuronal replacement in adult rat hippocampus after status epilepticus despite chronic inflammation. Eur J Neurosci 23:965–974. CrossRef Medline

Butovsky O, Talpalar AE, Ben-Yaakov K, Schwartz M (2005) Activation of microglia by aggregated beta-amyloid or lipopolysaccharide impairs MHC-II expression and renders them cytotoxic whereas IFN-gamma and IL-4 render them protective. Mol Cell Neurosci 29:381–393. CrossRef Medline

Butovsky O, Ziv Y, Schwartz A, Landa G, Talpalar AE, Pluchino S, Martino G, Schwartz M (2006a) Microglia activated by IL-4 or IFN-gamma differentially induce neurogenesis and oligodendrogenesis from adult stem/progenitor cells. Mol Cell Neurosci 31:149–160. CrossRef Medline

Butovsky O, Landa G, Kunis G, Ziv Y, Avidan H, Greenberg N, Schwartz A, Smirnov I, Pollack A, Jung S, Schwartz M (2006b) Induction and blockage of oligodendrogenesis by differently activated microglia in an animal model of multiple sclerosis. J Clin Invest 116:905–915. CrossRef Medline

Cacci E, Ajmone-Cat MA, Anelli T, Biagioni S, Minghetti L (2008) In vitro neuronal and glial differentiation from embryonic or adult neural precursor cells are differently affected by chronic or acute activation of microglia. Glia 56:412–425. CrossRef Medline

Camacho-Arroyo I, López-Griego L, Morales-Montor J (2009) The role of cytokines in the regulation of neurotransmission. Neuroimmunomodulation 16:1–12. CrossRef Medline

Cunningham CL, Martínez-Cerdeño V, Noctor SC (2013) Microglia regulate the number of neural precursor cells in the developing cerebral cortex. J Neurosci 33:4216–4233. CrossRef Medline

Das S, Basu A (2008) Inflammation: a new candidate in modulating adult neurogenesis. J Neurosci Res 86:1199–1208. CrossRef Medline

Deierborg T, Roybon L, Inacio AR, Pesic J, Brundin P (2010) Brain injury activates microglia that induce neural stem cell proliferation ex vivo and promote differentiation of neurosphere-derived cells into neurons and oligodendrocytes. Neuroscience 171:1386–1396. CrossRef Medline

Doetsch F, Scharff C (2001) Challenges for brain repair: insights from adult neurogenesis in birds and mammals. Brain Behav Evol 58:306–322. CrossRef Medline

Doetsch F, García-Verdugo JM, Alvarez-Buylla A (1999) Regeneration of a germinal layer in the adult mammalian brain. Proc Natl Acad Sci U S A 96:11619–11624. CrossRef Medline

Ekdahl CT (2012) Microglial activation- tuning and pruning adult neurogenesis. Front Pharmacol 3:41. CrossRef Medline

Ekdahl CT, Claasen JH, Bonde S, Kokaia Z, Lindvall O (2003) Inflammation is detrimental for neurogenesis in adult brain. Proc Natl Acad Sci U S A 100:13632–13637. CrossRef Medline

Ekdahl CT, Kokaia Z, Lindvall O (2009) Brain inflammation and adult neurogenesis: the dual role of microglia. Neuroscience 158:1021–1029. CrossRef Medline

Ginhoux F, Greter M, Leboeuf M, Nandi S, See P, Gokhan S, Mehler MF, Conway SJ, Ng LG, Stanley ER, Samokhvalov IM, Merad M (2010) Fate mapping analysis reveals that adult microglia derive from primitive macrophages. Science 330:841–845. CrossRef Medline

Goings GE, Kozlowski DA, Szele FG (2006) Differential activation of microglia in neurogenic versus non-neurogenic regions of the forebrain. Glia 54:329–342. CrossRef Medline

Gould E, Reeves AJ, Graziano MS, Gross CG (1999) Neurogenesis in the neocortex of adult primates. Science 286:548–552. CrossRef Medline

Hamanoue M, Matsuzaki Y, Sato K, Okano HJ, Shibata S, Sato I, Suzuki S, Ogawara M, Takamatsu K, Okano H (2009) Cell surface N-glycans mediated isolation of mouse neural stem cells. J Neurochem 110:1575–1584. CrossRef Medline

Hanisch UK, Kettenmann H (2007) Microglia: active sensor and versatile effector cells in the normal and pathologic brain. Nat Neurosci 10:1387–1394. CrossRef Medline

Hirasawa T, Ohsawa K, Imai Y, Ondo Y, Akazawa C, Uchino S, Kohsaka S (2005) Visualization of microglia in living tissues using Iba1-EGFP transgenic mice. J Neurosci Res 81:357–362. CrossRef Medline

Ignácio AR, Müller YM, Carvalho MS, Nazari EM (2005) Distribution of microglial cells in the cerebral hemispheres of embryonic and neonatal chicks. Braz J Med Biol Res 38:1615–1621. Medline

Inoue K (2008) Purinergic systems in microglia. Cell Mol Life Sci 65:3074–3080. CrossRef Medline

Iosif RE, Ekdahl CT, Ahlenius H, Pronk CJ, Bonde S, Kokaia Z, Jacobsen SE, Lindvall O (2006) Tumor necrosis factor receptor 1 is a negative regulator of progenitor proliferation in adult hippocampal neurogenesis. J Neurosci 26:9703–9712. CrossRef Medline

Islam O, Gong X, Rose-John S, Heese K (2009) Interleukin-6 and neural stem cells: more than gliogenesis. Mol Biol Cell 20:188–199. CrossRef Medline

Kettenmann H, Hanisch UK, Noda M, Verkhratsky A (2011) Physiology of microglia. Physiol Rev 91:461–553. CrossRef Medline

Koo JW, Duman RS (2008) IL-1beta is an essential mediator of the antineurogenic and anhedonic effects of stress. Proc Natl Acad Sci U S A 105:751–756. CrossRef Medline

Li L, Walker TL, Zhang Y, Mackay EW, Bartlett PF (2010) Endogenous interferon gamma directly regulates neural precursors in the non-inflammatory brain. J Neurosci 30:9038–9050. CrossRef Medline

Lie DC, Song H, Colamarino SA, Ming GL, Gage FH (2004) Neurogenesis in the adult brain: new strategies for central nervous system diseases. Annu Rev Pharmacol Toxicol 44:399–421. CrossRef Medline

Marshall GP 2nd, Demir M, Steindler DA, Laywell ED (2008) Subventricular zone microglia possess a unique capacity for massive in vitro expansion. Glia 56:1799–1808. CrossRef Medline

Miller RJ, Jung H, Bhangoo SK, White FA (2009) Cytokine and chemokine regulation of sensory neuron function. Handb Exp Pharmacol 194:417–449. CrossRef Medline

Miron VE, Boyd A, Zhao JW, Yuen TJ, Ruckh JM, Shadrach JL, van Wijngaarden P, Wagers AJ, Williams A, Franklin RJ, ffrench-Constant C (2013) M2 microglia and macrophages drive oligodendrocyte differentiation during CNS remyelination. Nat Neurosci 16:1211–1218. CrossRef Medline

Mohri I, Eguchi N, Suzuki K, Urade Y, Taniike M (2003) Hematopoietic prostaglandin D synthase is expressed in microglia in the developing postnatal mouse brain. Glia 42:263–274. CrossRef Medline

Monje ML, Toda H, Palmer TD (2003) Inflammatory blockade restores adult hippocampal neurogenesis. Science 302:1760–1765. CrossRef Medline

Monji A, Kato T, Kanba S (2009) Cytokines and schizophrenia: microglia

hypothesis of schizophrenia. Psychiatry Clin Neurosci 63:257–265. CrossRef Medline

Mosher KI, Andres RH, Fukuhara T, Bieri G, Hasegawa-Moriyama M, He Y, Guzman R, Wyss-Coray T (2012) Neural progenitor cells regulate microglia functions and activity. Nat Neurosci 15:1485–1487. CrossRef Medline

Nakajima K, Kohsaka S (2001) Microglia: activation and their significance in the central nervous system. J Biochem 130:169–175. CrossRef Medline

Nakajima K, Tsuzaki N, Shimojo M, Hamanoue M, Kohsaka S (1992) Microglia isolated from rat brain secrete a urokinase-type plasminogen activator. Brain Res 577:285–292. CrossRef Medline

Nakanishi M, Niidome T, Matsuda S, Akaike A, Kihara T, Sugimoto H (2007) Microglia-derived interleukin-6 and leukaemia inhibitory factor promote astrocytic differentiation of neural stem/progenitor cells. Eur J Neurosci 25:649–658. CrossRef Medline

Nishiyama A, Komitova M, Suzuki R, Zhu X (2009) Polydendrocytes (NG2 cells): multifunctional cells with lineage plasticity. Nat Rev Neurosci 10: 9–22. CrossRef Medline

Oh J, McCloskey MA, Blong CC, Bendickson L, Nilsen-Hamilton M, Sakaguchi DS (2010) Astrocyte-derived interleukin-6 promotes specific neuronal differentiation of neural progenitor cells from adult hippocampus. J Neurosci Res 88:2798–2809. CrossRef Medline

Ortega F, Gascón S, Masserdotti G, Deshpande A, Simon C, Fischer J, Dimou L, Chichung Lie D, Schroeder T, Berninger B (2013) Oligodendrogliogenic and neurogenic adult subependymal zone neural stem cells constitute distinct lineages and exhibit differential responsiveness to Wnt signalling. Nat Cell Biol 15:602–613. CrossRef Medline

Pont-Lezica L, Béchade C, Belarif-Cantaut Y, Pascual O, Bessis A (2011) Physiological roles of microglia during development. J Neurochem 119: 901–908. CrossRef Medline

Reynolds BA, Tetzlaff W, Weiss S (1992) A multipotent EGF-responsive striatal embryonic progenitor cell produces neurons and astrocytes. J Neurosci 12:4565–4574. Medline

Russo I, Barlati S, Bosetti F (2011) Effects of neuroinflammation on the regenerative capacity of brain stem cells. J Neurochem 116:947–956. CrossRef Medline

Schäfers M, Sorkin L (2008) Effect of cytokines on neuronal excitability. Neurosci Lett 437:188–193. CrossRef Medline

Spedding M, Gressens P (2008) Neurotrophins and cytokines in neuronal plasticity. Novartis Found Symp 289:222–233; discussion 233–240. Medline

Spooren A, Kolmus K, Laureys G, Clinckers R, De Keyser J, Haegeman G, Gerlo S (2011) Interleukin-6, a mental cytokine. Brain Res Rev 67:157–183. CrossRef Medline

Suzuki SO, Goldman JE (2003) Multiple cell populations in the early postnatal subventricular zone take distinct migratory pathways: a dynamic study of glial and neuronal progenitor migration. J Neurosci 23:4240–4250. Medline

Temple S (2001) The development of neural stem cells. Nature 414:112–117. CrossRef Medline

Thored P, Heldmann U, Gomes-Leal W, Gisler R, Darsalia V, Taneera J, Nygren JM, Jacobsen SE, Ekdahl CT, Kokaia Z, Lindvall O (2009) Long-term accumulation of microglia with proneurogenic phenotype concomitant with persistent neurogenesis in adult subventricular zone after stroke. Glia 57:835–849. CrossRef Medline

Tikka T, Fiebich BL, Goldsteins G, Keinanen R, Koistinaho J (2001) Minocycline, a tetracycline derivative, is neuroprotective against excitotoxicity by inhibiting activation and proliferation of microglia. J Neurosci 21: 2580–2588. Medline

Tremblay MÈ, Stevens B, Sierra A, Wake H, Bessis A, Nimmerjahn A (2011) The role of microglia in the healthy brain. J Neurosci 31:16064–16069. CrossRef Medline

Vela JM, Molina-Holgado E, Arévalo-Martín A, Almazán G, Guaza C (2002) Interleukin-1 regulates proliferation and differentiation of oligodendrocyte progenitor cells. Mol Cell Neurosci 20:489–502. CrossRef Medline

Vukovic J, Colditz MJ, Blackmore DG, Ruitenberg MJ, Bartlett PF (2012) Microglia modulate hippocampal neural precursor activity in response to exercise and aging. J Neurosci 32:6435–6443. CrossRef Medline

Wagner JP, Black IB, DiCicco-Bloom E (1999) Stimulation of neonatal and adult brain neurogenesis by subcutaneous injection of basic fibroblast growth factor. J Neurosci 19:6006–6016. Medline

Walton NM, Sutter BM, Laywell ED, Levkoff LH, Kearns SM, Marshall GP 2nd, Scheffler B, Steindler DA (2006) Microglia instruct subventricular zone neurogenesis. Glia 54:815–825. CrossRef Medline

Wang X, Fu S, Wang Y, Yu P, Hu J, Gu W, Xu XM, Lu P (2007) Interleukin-1beta mediates proliferation and differentiation of multipotent neural precursor cells through the activation of SAPK/JNK pathway. Mol Cell Neurosci 36:343–354. CrossRef Medline

Wu CH, Wen CY, Shieh JY, Ling EA (1993) A quantitative study of the differentiation of microglial cells in the developing cerebral cortex in rats. J Anat 182:403–413. Medline

Xu J, Ling EA (1994) Studies of the distribution and functional roles of transitory amoeboid microglial cells in developing rat brain using exogenous horseradish peroxidase as a marker. J Hirnforsch 35:103–111. Medline

Zerlin M, Milosevic A, Goldman JE (2004) Glial progenitors of the neonatal subventricular zone differentiate asynchronously, leading to spatial dispersion of glial clones and to the persistence of immature glia in the adult mammalian CNS. Dev Biol 270:200–213. CrossRef Medline

Zhao C, Ling Z, Newman MB, Bhatia A, Carvey PM (2007) TNF-alpha knockout and minocycline treatment attenuates blood–brain barrier leakage in MPTP-treated mice. Neurobiol Dis 26:36–46. CrossRef Medline

Ziv Y, Ron N, Butovsky O, Landa G, Sudai E, Greenberg N, Cohen H, Kipnis J, Schwartz M (2006) Immune cells contribute to the maintenance of neurogenesis and spatial learning abilities in adulthood. Nat Neurosci 9:268–275. CrossRef Medline

Niflumic Acid Activates Additional Currents of the Human Glial L-Glutamate Transporter EAAT1 in a Substrate-Dependent Manner

Kanako Takahashi,[a] Reiko Ishii-Nozawa,[b] Koichi Takeuchi,[b] Ken Nakazawa,[a] Yuko Sekino,[a] and Kaoru Sato*,[a]

[a] *Laboratory of Neuropharmacology, Division of Pharmacology, National Institute of Health Sciences; 1–18–1 Kamiyoga, Setagaya, Tokyo 158–8501, Japan: and* [b] *Department of Clinical Pharmacology, Meiji Pharmaceutical University; 2–522–1 Noshio, Kiyose, Tokyo 204–8588, Japan.*
Received September 6, 2013; accepted September 29, 2013

The astrocytic L-glutamate (L-Glu) transporter EAAT1 participates in the removal of L-Glu from the synaptic cleft and maintenance of non-toxic concentrations in the extracellular fluid. We have shown that niflumic acid (NFA), a non-steroidal anti-inflammatory drug (NSAIDs), alters L-Glu-induced EAAT1 currents in a voltage-dependent manner using the two-electrode voltage clamp technique in *Xenopus* oocytes expressing EAAT1. In this study, we characterised the effects of NFA on each type of ion-flux through EAAT1. NFA modulated currents induced by both L-Glu and L-aspartate (L-Asp) in a voltage-dependent manner. Ion-substitution experiments revealed that the activation of additional H^+ conductance was involved in the modulation of currents induced by L-Asp and L-Glu, but Cl^- was involved only with the L-Asp currents. NFA activated additional currents of EAAT1 in a substrate-dependent manner.

Key words astrocytic L-glutamate transporter; niflumic acid; additional conductance; EAAT1; voltage-dependent manner

Neuronal and astrocytic L-glutamate (L-Glu) transporters (EAATs) are the only significant machinery for the removal of L-Glu from the synaptic cleft and maintenance of non-toxic concentrations in the extracellular fluid.[1] Along with controlling extracellular L-Glu concentrations, EAATs also play a role in the regulation of functional crosstalk between neurons and glial cells by modulating the ion flux. L-Glu is co-transported into a cell with 3 Na^+ and 1 H^+ by EAATs, followed by the counter-transport of 1 K^+ [2]. L-Glu and Na^+ binding to EAATs activates a non-stoichiometrically-coupled (uncoupled) Cl^- conductance.[3] The Na^+ influx triggers functional metabolic crosstalk between neurons and astrocytes,[4] and the uncoupled Cl^- conductance dampens neuronal excitability.[5,6]

Niflumic acid [2-((3-(trifluoromethyl)phenyl)amino)-3-pyridinecarboxylic acid, NFA], a member of a class of non-steroidal anti-inflammatory drugs (NSAIDs), modulates the gating of Cl^- channels,[7,8] K^+ channels,[9–14] nicotinic acetylcholine channels,[15] and transient receptor potential channels.[16] NFA also enhances the substrate-gated currents of EAAT4, an L-Glu transporter expressed primarily in Purkinje neurons,[17] by activating additional uncoupled H^+ and Cl^- conductances.[18] We recently discovered that NFA modulates the current mediated through EAAT1, an astrocytic L-Glu transporter,[19,20] in a voltage-dependent manner.[21] In this study, we characterised the effects of NFA on L-Glu and L-aspartate (L-Asp) currents, focusing on each ion-flux. We report here that the activation of additional H^+ conductance was involved in the modulation by NFA of both L-Glu currents and L-Asp currents, whereas Cl^- was involved only in the modulation of L-Asp currents.

MATERIALS AND METHODS

Expression of EAAT1 in *Xenopus* Oocytes All of the animals were treated in accordance with the guidelines for the Care and Use of Laboratory Animals of the Animal Research Committee of the National Institute of Health Sciences, Japan. A pcDNA3.1 plasmid containing the cDNA of the human glutamate transporter EAAT1 was obtained from Dr. Keiko Shimamoto (Suntory Institute for Bioorganic Research, Osaka, Japan). The plasmids containing the EAAT1 cDNA were linearized at a *Not*I (Toyobo, Osaka, Japan) site, and capped RNA was transcribed from the linearized cDNA construct with a bacteriophage T7 RNA polymerase (mMESSAGE mMACHINE; Ambion, Austin, TX, U.S.A.). Oocytes were collected from anaesthetised *Xenopus laevis*. The isolated oocytes were then treated with collagenase (2 mg mL^{-1}, type 1, Sigma, St. Louis, MO, U.S.A.), and capped mRNA was injected into either defolliculated stage V or VI oocytes. The oocytes were incubated for 2–7 d at 18°C in ND96 solution containing 96 mM NaCl, 2 mM KCl, 1.8 mM $CaCl_2$, 1 mM $MgCl_2$, and 5 mM *N*-(2-hydroxyethyl)piperazine-*N'*-(2-ethanesulfonic acid) (HEPES) (pH 7.5) supplemented with 0.01% gentamycin.

Electrophysiology Two-electrode voltage clamp recordings from EAAT1-expressing oocytes were performed at room temperature (25–27°C) using glass microelectrodes filled with 3 M KCl solution (resistance=1–4 MΩ) and an Ag/AgCl pellet bath ground (EP2; World Precision Instruments, Sarasota, FL, U.S.A.). A bath-clamp amplifier (OC-725C; Warner Instruments, Hamden, CT, U.S.A.) was used with a Digidata 1320A interface (Axon Instruments, Foster City, CA, U.S.A.). The pClamp suite of programs (ver. 8.2; Axon Instruments) and the Clampfit data acquisition software were used to control stimulation parameters, and to acquire and analyse data. An Ag/AgCl pellets were used to avoid voltage errors associated with buffer changes. Oocytes were continuously superfused with ND96 solution. To adjust the extracellular H^+ to various concentrations, the HEPES was replaced by either 2-(*N*-morpholino)ethanesulfonic acid (MES) (pH 5.5, 6.5) or [(2-hydroxy-1,1-bis(hydroxymethyl)ethyl)amino]-1-propanesulfonic acid (TAPS) (pH 8.5). For Na^+ substitution experiments, Na^+ was replaced by equimolar choline ions. For

The authors declare no conflict of interest.

* To whom correspondence should be addressed. e-mail: kasato@nihs.go.jp

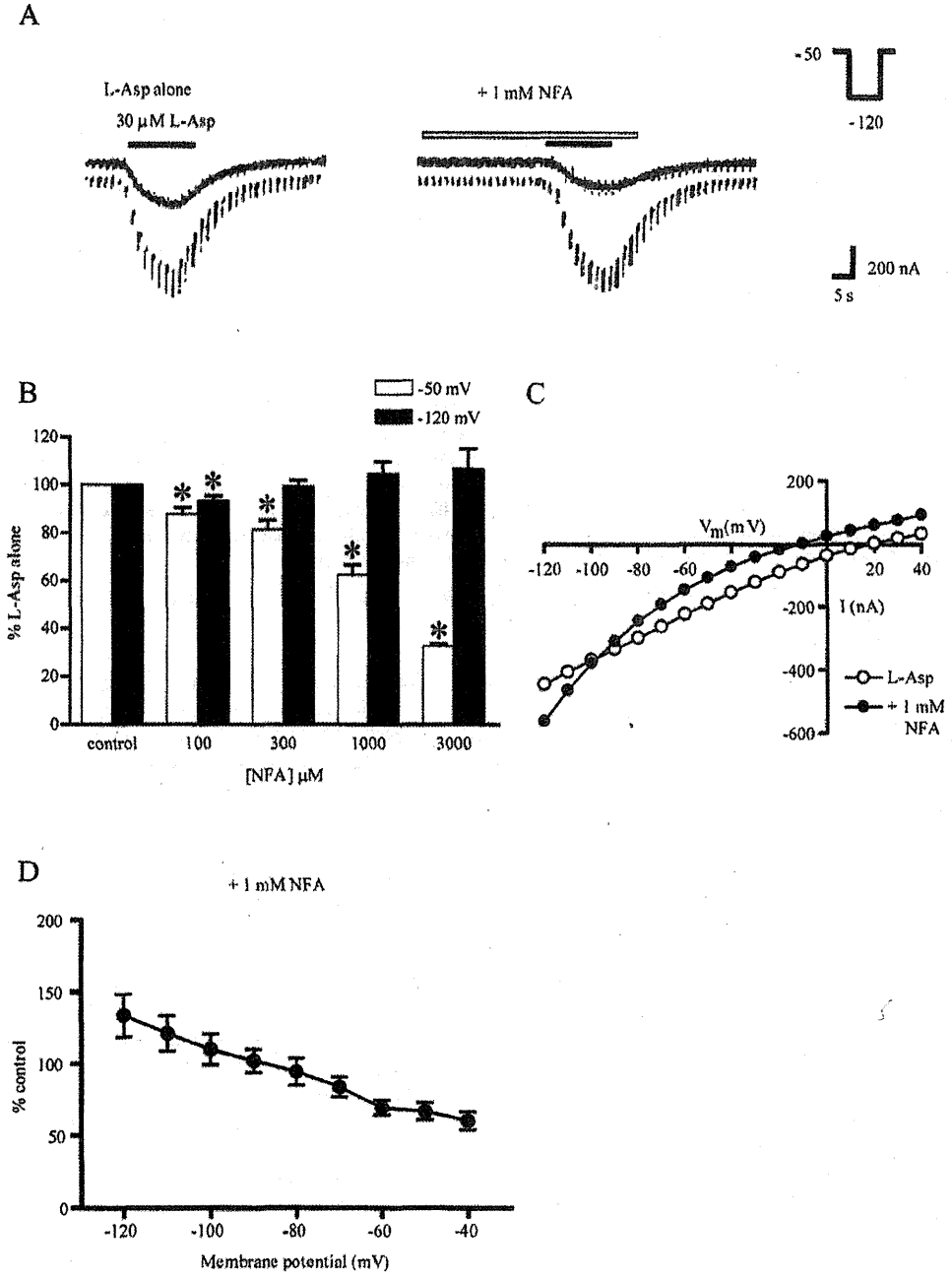

Fig. 1. Niflumic Acid (NFA) Modulated L-Asp-Induced Currents in *Xenopus* Oocytes Expressing EAAT1 in a Voltage-Dependent Manner

A: The traces of L-Asp (30 μM)-induced inward currents in either the absence or presence of NFA (1 mM) at −50 mV (bold line) and −120 mV (thin line). The oocytes were held at −50 mV and hyperpolarised to −120 mV for 400 ms every 2 s. B: Concentration–response relationships of the effects of NFA on L-Asp currents at −50 mV and −120 mV. The effects of NFA on the peak amplitude of the L-Asp current were examined by comparing the current in the presence of NFA to that recorded just prior to the drug treatment (control response) at each concentration. Data are analysed by paired *t*-test. Graph shows the summary of the results. Each column shows the averaged data normalized to the control (4–5 oocytes for each) at each concentration. At −50 mV, NFA inhibited the peak amplitudes of the L-Asp currents in a concentration-dependent manner, whereas NFA only slightly increased the peak amplitude of the L-Asp-induced currents at −120 mV. $*p<0.05$ *vs.* control. C: Representative current–voltage relationships for L-Asp (30 μM) in either the absence or presence of NFA (1 mM). The current–voltage relationships were obtained with a holding potential of −50 mV and implementation of 400-ms voltage jumps in 10 mV increments over the range from −120 mV to +40 mV. For the control, the current values at steady state were subtracted from those measured in the presence of L-Asp. For the NFA-treated group, the current values in the presence of NFA alone were subtracted from those in the presence of both NFA and L-Asp. NFA treatment produced a leftward shift of E_{rev} (from 18.4±5.4 to −2.7±4.1 mV; $n=10$, $p<0.05$, paired *t*-test). D: The relationship between the effects and the holding potential. The current in the presence of NFA was normalized to that obtained just before the application of NFA. The effects of NFA was voltage-dependent ($n=10$).

the Cl^- substitution experiments, Cl^- was replaced by equimolar gluconate ions. Oocytes were bathed in an experimental chamber (0.5 mL) filled with ND96 solution and voltage-clamped at −50 mV. A 400 ms hyperpolarising voltage step to −120 mV was applied every 2 s to confirm clamp conditions and observe the voltage dependence of current responses. As

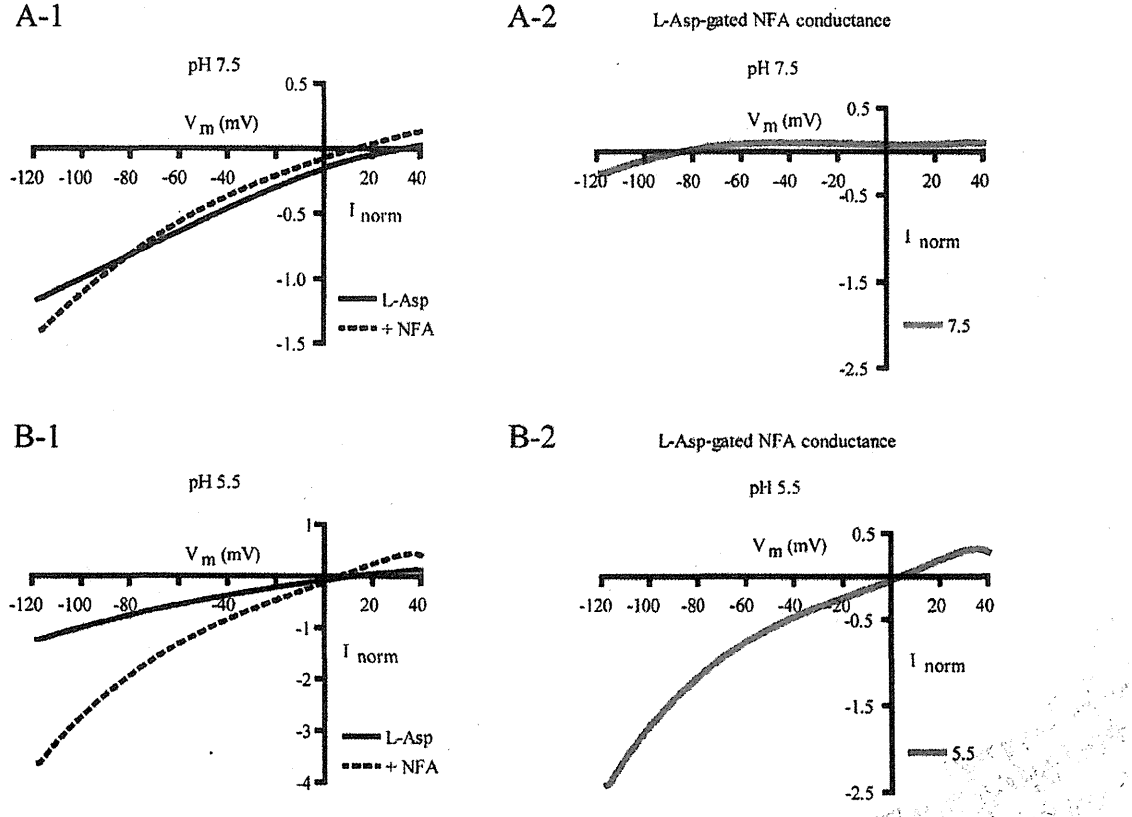

Fig. 2. Influence of Extracellular pH on L-Asp Currents in Either the Absence or Presence of NFA

The current–voltage relationships were determined using a holding potential of −50 mV and implementing an 800 ms ramp pulse over the range from +40 mV to −120 mV. The current–voltage relationships for the L-Asp-gated NFA-induced conductance were obtained by subtracting the control L-Asp currents from the L-Asp currents in the presence of NFA. The currents are normalised to the amplitude of the L-Asp currents generated at −100 mV. A-1 and B-1: Average current–voltage relationships for L-Asp (30 μM) in either the absence (solid line) or presence (dotted line) of NFA (300 μM) at pH 7.5 (A-1) and pH 5.5 (B-1). A-2 and B-2: Average current–voltage relationships for the L-Asp-gated NFA-induced conductance at pH 7.5 (A-2) and pH 5.5 (B-2). The average shift of the sub-E_{rev} was −45.1±4.0 mV per pH unit, which is consistent with that reported for H^+-selective channels. Each point represents the mean value from 5 oocytes.

a substrate, 30 μM of either L-Glu or L-Asp (half of the EC_{50}) was applied to the oocytes by superfusion at 0.2 mL·s^{-1} of constant flow rate for 15 s with regular 30 s intervals. NFA was applied from 30 s before to 5 s after the end of the application of substrate. The current–voltage relationships for substrate transport were determined by subtracting the steady-state currents obtained with a holding potential of −50 mV either implementing 400 ms voltage jumps in 10 mV increments from −120 to +60 mV or implementing an 800 ms ramp pulse from −120 to +40 mV in the absence of substrate from the corresponding currents in the presence of substrate. The currents are normalised to the amplitude of the L-Asp or L-Glu currents generated at −100 mV (Figs. 2–8).

Preparation of the Compounds All chemicals were purchased from Wako (Tokyo, Japan) unless otherwise stated. NFA, TAPS, and MES were purchased from Sigma (St. Louis, MO, U.S.A.). L-Asp and L-Glu stock solutions (20 mM) were made in purified water (Millipore, Billerica, MA, U.S.A.). The NFA stock solution (300 mM) was made in dimethyl sulfoxide (DMSO) and dissolved in ND96 solution immediately prior to each experiment. The pH of every solution was adjusted to 7.5, and the final concentrations of the solvents were less than 1%.

Statistical Analysis All of the data are presented as the mean±S.E.M. p Values were obtained by statistical analysis, as noted in the figure legends.

RESULTS

Effects of NFA on L-Asp-Induced Currents in *Xenopus* Oocytes Expressing EAAT1 We first examined the effects of NFA on the L-Asp-induced currents in *Xenopus* oocytes expressing EAAT1. The left trace in Fig. 1A represents the inward control current produced by L-Asp (30 μM) voltage clamped at −50 mV with 400 ms hyperpolarising voltage steps to −120 mV every 2 s. At −50 mV, NFA (300 μM–3 mM) inhibited the peak amplitude of the L-Asp-induced currents in a concentration-dependent manner, whereas at 120 mV, NFA only slightly increased the peak amplitude of the L-Asp-induced currents (Figs. 1A, B). Figure 1C shows the representative current–voltage relationships for L-Asp (30 μM)-induced currents in either the presence or absence of 1 mM NFA. In the absence of NFA, the L-Asp current was linear in a voltage-dependent manner, with the reversal potential (E_{rev}) at 18.4±5.4 mV. NFA treatment resulted in a leftward shift of the E_{rev} of the L-Asp currents (from 18.4±5.4 to −2.7±4.1 mV; n=10, p<0.05, paired t-test). The current–voltage curve recorded in the presence of NFA crossed the control curve at

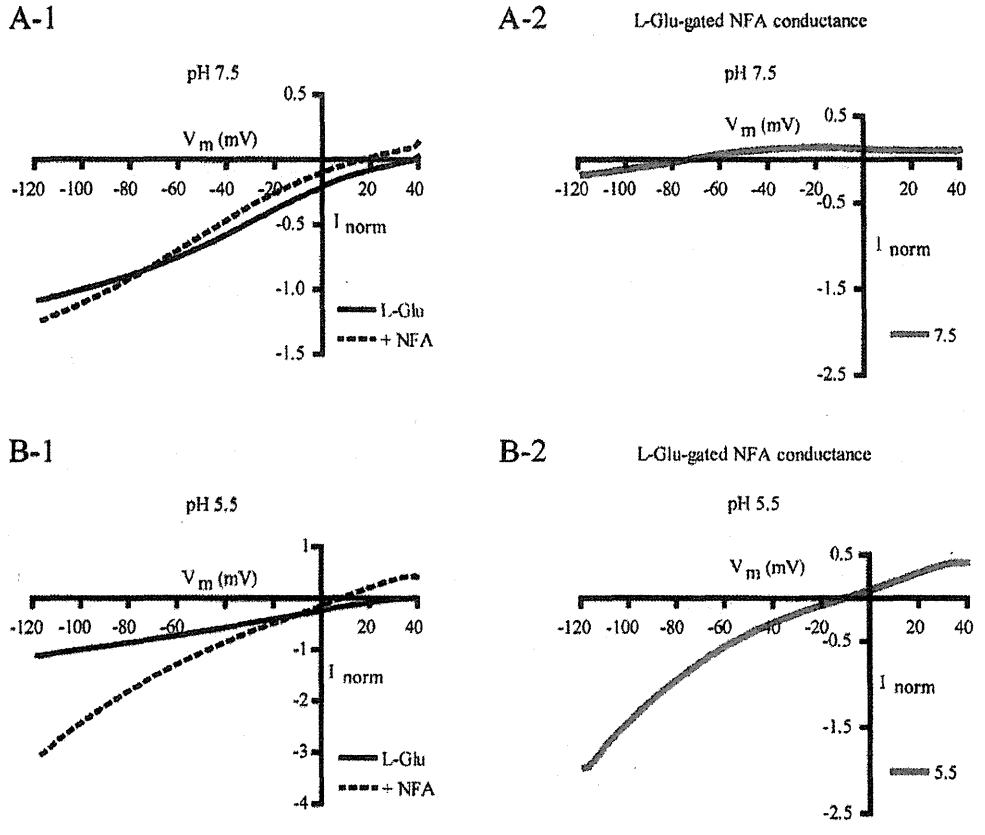

Fig. 3. Influence of Extracellular pH on L-Glu Currents in Either the Absence or Presence of NFA

A-1 and B-1: Average current–voltage relationships for L-Glu (30 μM) in either the absence (solid line) or presence (dotted line) of NFA (300 μM) at pH 7.5 (A-1) and pH 5.5 (B-1). A-2 and B-2: Average current–voltage relationships for the L-Glu-gated NFA-induced conductance at pH 7.5 (A-2) and pH 5.5 (B-2). The average shift of the sub-E_{rev} was −36.6±4.6 mV per pH unit, which is consistent with that reported for H^+-selective channels. Each point represents the mean value from 5 oocytes.

−96.5 mV (cross-over potential), indicating that NFA inhibited the L-Asp currents at potentials more positive than −96.5 mV and increased the currents at potentials more negative than −96.5 mV. The influence of NFA on the peak current amplitude was voltage-dependent (Fig. 1D). This voltage-dependent effect of NFA has also been observed with L-Glu current in our previous study.[21]

Involvement of Additional H^+ Conductance We examined whether any additional H^+ conductance is involved in these voltage-dependent effect of NFA. The effects of NFA were examined when the extracellular pH was 7.5 and 5.5. Figures 2A-1 and B-1 show the average current–voltage relationships for the L-Asp current (30 μM) in either the absence (solid line) or presence (dotted line) of NFA (300 μM) at pH 7.5 (Fig. 2A-1) and pH 5.5 (Fig. 2B-1). At pH 7.5, the curve of the L-Asp current in the presence of NFA crossed the control curve at −84 mV, whereas the crossover potential was at +4 mV at pH 5.5. The L-Asp-gated NFA-induced conductance was obtained by subtracting the L-Asp current from the L-Asp current in the presence of NFA (Figs. 2A-2, B-2). As the extracellular H^+ concentration increased, the E_{rev} of the L-Asp-gated NFA-induced conductance (sub-E_{rev}) shifted toward the more positive membrane potential. The average shift of the sub-E_{rev} gated by L-Asp was −45.1±4.0 mV per pH unit (n=5), which is consistent with previous reports for H^+-selective channels,[22,23] suggesting that NFA promotes additional H^+ conductance. Regarding L-Glu currents (Fig. 3), as the extracellular H^+ concentrations increased, the crossover potential shifted toward the more positive potential (Figs. 3A-1, B-1), and the sub-E_{rev} also shifted toward a more positive membrane potential (Figs. 3A-2, B-2). The average shift of the sub-E_{rev} gated by L-Glu changed −36.6±4.6 mV per pH unit (n=5), suggesting that NFA promotes additional H^+ conductance in this case as well. There were no significant differences between the average shifts of the sub-E_{rev} per pH unit gated by L-Asp and L-Glu (Student's t-test, p=0.2).

Involvement of Additional Na^+ Conductance We examined if the additional Na^+ conductance is involved in these voltage-dependent effect of NFA. The current–voltage relationships for the L-Asp current in either the absence or presence of NFA were examined under various extracellular [Na^+] by choline substitution. Figures 4A-1 and B-1 show the average current–voltage relationships for L-Asp in either the absence (solid line) or presence (dotted line) of NFA (300 μM) at normal [Na^+] (96 mM) (Fig. 4A-1) and low [Na^+] (24 mM) (Fig. 4B-1). Decreasing the extracellular [Na^+] resulted in a loss of crossover between −120 mV and +40 mV, indicating that low extracellular [Na^+] results in a loss of the voltage-dependent modulation of L-Asp currents by NFA. The L-Asp-gated NFA-induced conductance-voltage relationships displayed inward rectification with the sub-E_{rev} at −58 mV (Fig. 4A-2) at normal [Na^+], whereas no significant subtracted currents

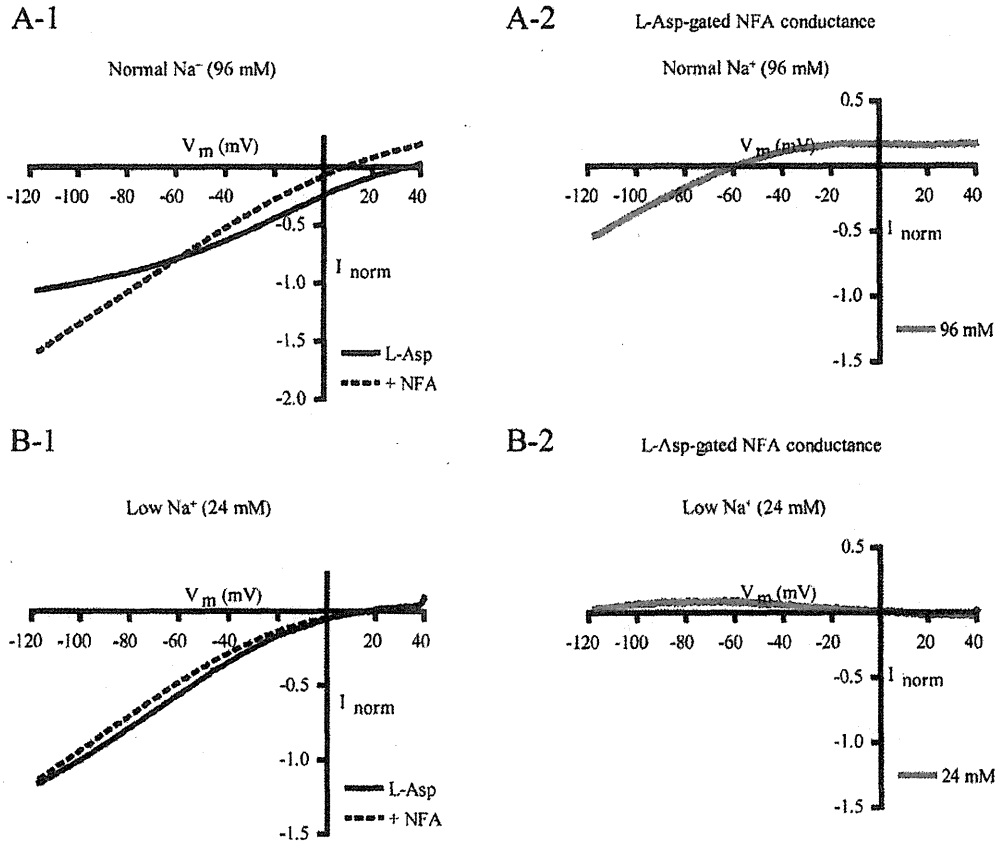

Fig. 4. Influence of Extracellular [Na^+] on L-Asp-Gated NFA-Induced Conductance and the L-Asp Currents in Either the Absence or Presence of NFA

The current–voltage relationships for the L-Asp current in either the absence or presence of NFA were examined under various extracellular [Na^+] by choline substitution. A-1 and B-1: Average current–voltage relationships for L-Asp (30 μM) in either the absence (solid line) or presence (dotted line) of NFA (300 μM) at normal [Na^+] (96 mM) (A-1) and low [Na^+] (24 mM) (B-1). A-2 and B-2: Average current–voltage relationships for the L-Asp-gated NFA-induced conductance at normal [Na^+] (96 mM) (A-2) and low [Na^+] (24 mM) (B-2). The average shift of the sub-E_{rev} gated by L-Asp was -1.1 ± 12.4 mV (n=3) per 10-fold change in [Na^+]. Each point represents the mean from 3 oocytes.

were observed at low [Na^+], suggesting that the modulation of L-Asp currents by NFA depends on the extracellular Na^+ concentration. Comparing the sub-E_{rev} at normal [Na^+] (96 mM) with that at middle-low [Na^+] (48 mM), the average shift of the sub-E_{rev} gated by L-Asp was -1.1 ± 12.4 mV (n=3) per 10-fold change in [Na^+]. In the case of L-Glu, decreasing the extracellular [Na^+] also resulted in a loss of crossover between -120 mV and $+40$ mV (Figs. 5A-1, B-1). The sub-E_{rev} gated by L-Glu was -68 mV at normal [Na^+], whereas no significant subtracted currents were observed at low [Na^+] (Figs. 5A-2, B-2), suggesting that the voltage-dependent modulation of L-Glu currents by NFA depends on the extracellular Na^+ concentration. Comparing the sub-E_{rev} at normal [Na^+] with that at middle-low [Na^+], the average shift of the sub-E_{rev} gated by L-Glu was 7.8 ± 2.2 mV (n=3) per 10-fold change in [Na^+]. This value was not significantly different from that for L-Asp (Student's t-test, p=0.5).

Involvement of Additional Cl^- Conductance Finally, we examined the contribution of additional Cl^- conductance. The current–voltage relationships for the L-Asp current in either the absence or presence of NFA were examined under various extracellular [Cl^-] by gluconate substitution. Figures 6A-1 and B-1 show the average current–voltage relationships for L-Asp in either the absence (solid line) or presence (dotted line) of NFA (300 μM) at normal [Cl^-] (103 mM) (Fig. 6A-1) and low [Cl^-] (30 mM) (Fig. 6B-1). At low [Cl^-], the crossover potential shifted toward the more negative potential (from -61 mV to -115 mV) and the sub-E_{rev} also shifted toward the more negative membrane potential. The average shift of the sub-E_{rev} gated by L-Asp was 94.9 ± 6.7 mV per 10-fold change in [Cl^-] (n=4) (Fig. 6C), indicating that Cl^- contributes to the L-Asp-gated NFA-induced conductance. Regarding L-Glu currents, no changes were observed in the crossover potential at low [Cl^-] (Figs. 7A-1, B-1) and a small shift of the sub-E_{rev} gated by L-Glu occurred at low [Cl^-] (Figs. 7A-2, B-2). The average shift of the sub-E_{rev} gated by L-Glu was 1.9 ± 8.1 mV per 10-fold change in [Cl^-] (n=4) (Fig. 7C), indicating that little contribution of Cl^- to the L-Glu-gated NFA-induced conductance. The significant difference in the additional Cl^- conductance between the L-Asp current and L-Glu current (Student's t-test, $p<0.05$) suggests that mechanisms for the modulation of EAAT1 currents by NFA is substrate-dependent.

DISCUSSION

In this study, we observed that the additional conductances

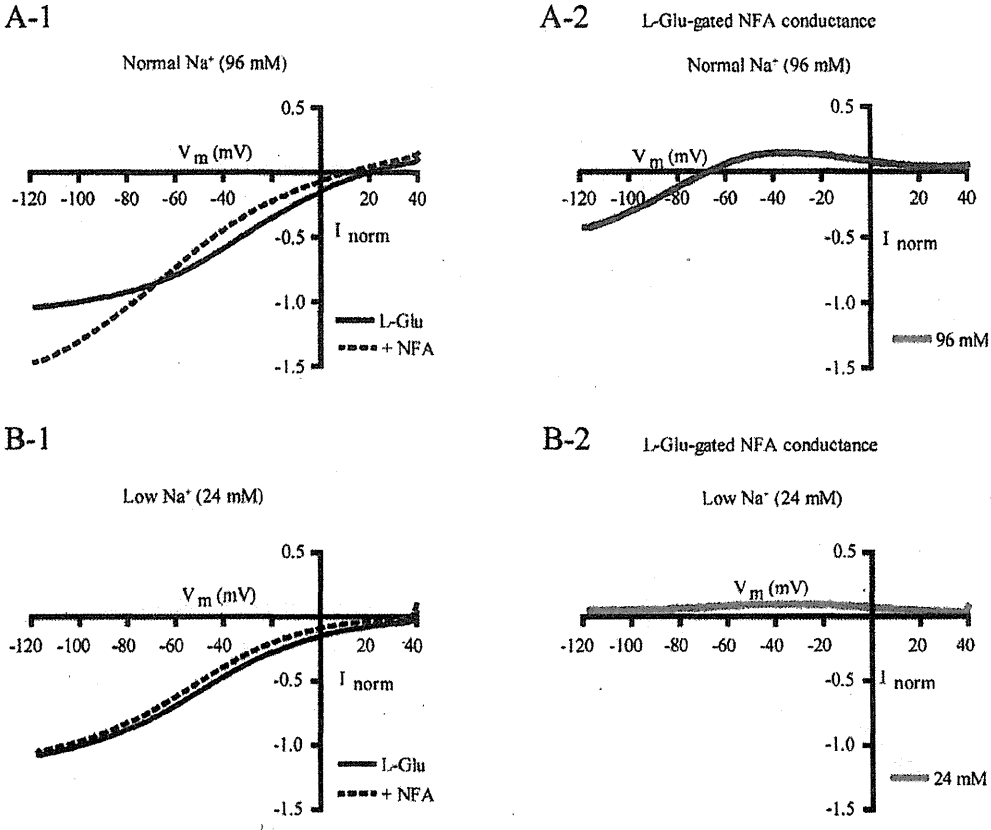

Fig. 5. Influence of Extracellular [Na^+] on L-Glu-Gated NFA-Induced Conductance and the L-Glu Currents in Either the Absence or Presence of NFA

A-1 and B-1: Average current–voltage relationships for L-Glu (30 μM) in either the absence (solid line) or presence (dotted line) of NFA (300 μM) at normal [Na^+] (96 mM) (A-1) and low [Na^+] (24 mM) (B-1). A-2 and B-2: Average current–voltage relationships for the L-Glu-gated NFA-induced conductance at normal [Na^+] (96 mM) (A-2) and low [Na^+] (24 mM) (B-2). The average shift of the sub-E_{rev} gated by L-Glu was 7.8±2.2 mV (n=3) per 10-fold change in [Na^+], which was statistically insignificant compared with that by L-Asp. Each point represents the mean from 5 oocytes.

of EAAT1 were activated when substrates were transported in the presence of NFA. Furthermore, the ionic contribution to the additional conductances is substrate dependent. To our knowledge, this is the first report showing the existence of additional conductances of EAAT1.

Poulsen and Vandenberg reported that NFA induced additional H^+ and Cl^- conductances in *Xenopus* oocytes expressing EAAT4, and these conductances were not thermodynamically coupled to the transport of substrates.[18] These conductances have been referred to as 'slippage.'[24] In our experiments using cultured astrocytes,[25] 300 μM of NFA significantly decreased the L-Glu uptake in cultured astrocytes (data not shown). Membrane potential of cultured astrocytes is approximately −74 mV.[26] Because the crossover potential of the L-Glu currents and NFA (300 μM)-gated L-Glu currents was −72.7±4.5 mV (n=12) in the present study, it is suggested that NFA-gated conductance observed here is not thermodynamically coupled to substrate transport, *i.e.*, NFA induces EAAT1 slippage as well. Transport experiments in voltage-clamped oocytes are necessary to confirm whether additional conductances in EAAT1 are not thermodynamically coupled to the substrate transport.

Sacher *et al.* presented a 'clutch' mechanism for slippage *via* the mammalian and yeast metal-ion transporter DCT1.[27] This mechanism could be explained in terms of two unique but interconnected ion pathways, one dominated by the ion utilized for driving the transport and the other by the transported metal ions. Loose coupling (namely clutching) between the driving force pathway and the metal ion transport pathway generates this observed slippage. Regarding EAAT1, in the presence of NFA, additional H^+ conductance may have arisen as a consequence of a subtle disruption to the ion binding sites, which compromises the coupling between the substrate transport pathway and the ion co-transport ($Na^+/H^+/K^+$) pathway. In support of this, a chimeric transporter generated with EAAT1 and EAAT2, whose junction site is in helical hairpin 2 and in close proximity to the substrate and Na^+ binding site, allows both Na^+ and K^+ to pass through the transporter in the absence of L-Glu.[28]

Interestingly, the ionic contribution is substrate-dependent, *i.e.*, the activation of additional H^+ conductance was involved in the modulation by NFA of both of L-Glu currents and L-Asp currents, whereas Cl^- was only involved in the modulation of L-Asp currents. Wadiche *et al.* reported that Cl^- permeation properties of EAAT1 were substrate-dependent, *i.e.*, the uncoupled Cl^- conductance per transport cycle gated by D-Asp was greater than that gated by L-Glu.[29] The mechanisms underlying the difference between L-Glu and L-Asp observed here may be related the one that causes the greater Cl^- by D-Asp. To elucidate the mechanisms, it is necessary to identify

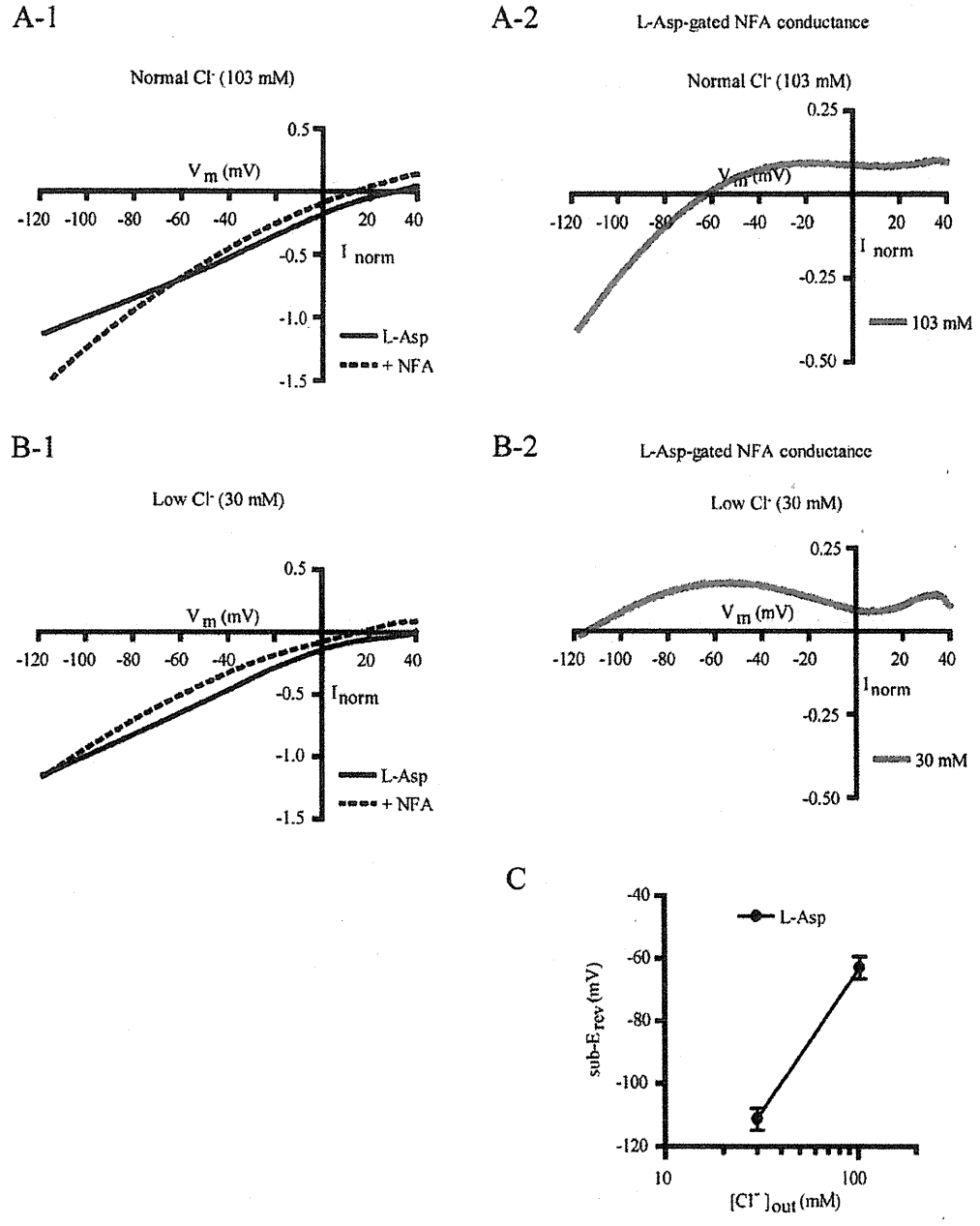

Fig. 6. Influence of Extracellular [Cl^-] on L-Asp-Gated NFA-Induced Conductance and the L-Asp Currents in Either the Absence or Presence of NFA

The current–voltage relationships for the L-Asp current in either the absence or presence of NFA were examined under various extracellular [Cl^-] by gluconate substitution. A-1 and B-1: Average current–voltage relationships for L-Asp (30 μM) in either the absence (solid line) or presence (dotted line) of NFA (300 μM) at normal [Cl^-] (103 mM) (A-1) and low [Cl^-] (30 mM) (B-1). A-2 and B-2: Average current–voltage relationships for the L-Asp-gated NFA-induced conductance at normal [Cl^-] (103 mM) (A-2) and low [Cl^-] (30 mM) (B-2). Each point represents the mean from 5 oocytes. C: Each point (filled circle) represents the mean sub-E_{rev} for L-Asp obtained in A-2 and B-2. Alterations in the extracellular Cl^- concentration caused average shifts of 94.9±6.7 mV per 10-fold change in [Cl^-] (n=4) in the sub-E_{rev}.

the binding site of NFA on EAAT1, and the stoichiometric interaction among the substrates, EAAT1, and NFA.

Alterations in the glial intracellular pH can induce a variety of changes in cellular function, *e.g.*, ionic currents, gap junction conductance, and enzymatic activities.[30] For example, in Bergmann glial cells, which highly express EAAT1,[19,20] electrical coupling *via* gap junctions has been shown to be modulated by altering intracellular pH.[31] Activation of additional H^+ conductance by NFA could be related to the effects of the drug in altering intracellular pH.

In conclusion, we observed substrate-dependent mechanisms for the modulation of EAAT1 currents by NFA. Activation of additional H^+ conductance was involved in the NFA-induced modulation of EAAT1 currents induced by L-Asp and L-Glu. The Cl^- ion was only involved in the NFA-induced modulation of L-Asp currents.

Acknowledgments We would like to thank Dr. Y. Yasu-

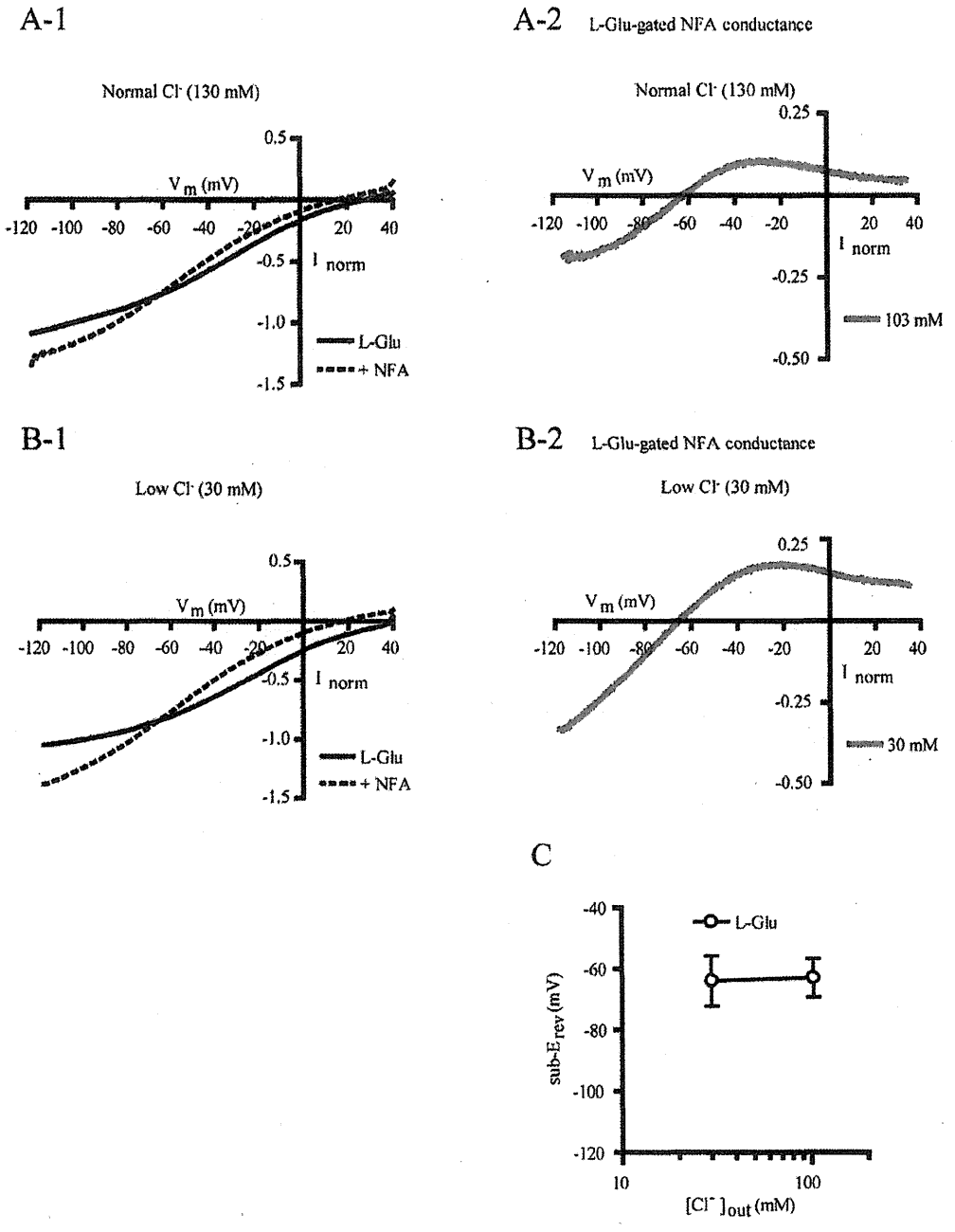

Fig. 7. Influence of Extracellular Cl^- on L-Glu-Gated NFA-Induced Conductance and the L-Glu Currents in Either the Absence or Presence of NFA

A-1 and B-1: Average current–voltage relationships for L-Glu (30 μM) in either the absence (solid line) or presence (dotted line) of NFA (300 μM) at normal [Cl^-] (103 mM) (A-1) and low [Cl^-] (30 mM) (B-1). A-2 and B-2: Average current–voltage relationships for the L-Glu-gated NFA-induced conductance at normal [Cl^-] (103 mM) (A-2) and low [Cl^-] (30 mM) (B-2). Each point represents the mean from 4 oocytes. C: Each point (open circle) represents the mean sub-E_{rev} for L-Glu obtained in A-2 and B-2. Alterations in the extracellular Cl^- concentrations caused average shifts of 1.9±8.1 mV per 10-fold change in [Cl^-] (n=4) in the sub-E_{rev}, which is significantly different from that of L-Asp (Student's t-test, $p<0.05$).

da-Kamatani and Dr. K. Shimamoto for providing the cDNA of EAAT1. We also thank Dr. T. Nakagawa and Dr. Y. Shigeri for their helpful suggestions. This work was partially supported by Grants-in-Aid for Young Scientists from the Ministry of Education, Culture, Sports, Science and Technology of Japan (KAKENHI 18700373, 21700422); Grant-in-Aid from the Food Safety Commission of Japan (No. 1003); the Program for the Promotion of Fundamental Studies in Health Sciences of NIBIO, Japan; a Health and Labour Science Research Grant for Research on Risks of Chemicals; and a Health and Labour Science Research Grant for Research on New Drug Development from MHLW, Japan; a Health and Labour Science Research Grant for Research on Risks of Chemicals from the MHLW, Japan; awarded to K.S. and a Health and Labour Science Research Grant for Research on New Drug Development from MHLW, Japan awarded to Y.S.

REFERENCES

1) Logan WJ, Snyder SH. Unique high affinity uptake systems for glycine, glutamic and aspartic acids in central nervous tissue of the rat. *Nature*, **234**, 297–299 (1971).
2) Zerangue N, Kavanaugh MP. Flux coupling in a neuronal glutamate transporter. *Nature*, **383**, 634–637 (1996).
3) Fairman WA, Vandenberg RJ, Arriza JL, Kavanaugh MP, Amara SG. An excitatory amino-acid transporter with properties of a ligand-gated chloride channel. *Nature*, **375**, 599–603 (1995).
4) Voutsinos-Porche B, Bonvento G, Tanaka K, Steiner P, Welker E, Chatton JY, Magistretti PJ, Pellerin L. Glial glutamate transporters mediate a functional metabolic crosstalk between neurons and astrocytes in the mouse developing cortex. *Neuron*, **37**, 275–286 (2003).
5) Veruki ML, Morkve SH, Hartveit E. Activation of a presynaptic glutamate transporter regulates synaptic transmission through electrical signaling. *Nat. Neurosci.*, **9**, 1388–1396 (2006).
6) Wersinger E, Schwab Y, Sahel JA, Rendon A, Pow DV, Picaud S, Roux MJ. The glutamate transporter EAAT5 works as a presynaptic receptor in mouse rod bipolar cells. *J. Physiol.*, **577**, 221–234 (2006).
7) White MM, Aylwin M. Niflumic and flufenamic acids are potent reversible blockers of Ca^{2+}-activated Cl^- channels in *Xenopus* oocytes. *Mol. Pharmacol.*, **37**, 720–724 (1990).
8) Scott-Ward TS, Li H, Schmidt A, Cai Z, Sheppard DN. Direct block of the cystic fibrosis transmembrane conductance regulator Cl^- channel by niflumic acid. *Mol. Membr. Biol.*, **21**, 27–38 (2004).
9) Ottolia M, Toro L. Potentiation of large conductance KCa channels by niflumic, flufenamic, and mefenamic acids. *Biophys. J.*, **67**, 2272–2279 (1994).
10) Busch AE, Herzer T, Wagner CA, Schmidt F, Raber G, Waldegger S, Lang F. Positive regulation by chloride channel blockers of IsK channels expressed in *Xenopus* oocytes. *Mol. Pharmacol.*, **46**, 750–753 (1994).
11) Wang HS, Dixon JE, McKinnon D. Unexpected and differential effects of Cl^- channel blockers on the Kv4.3 and Kv4.2 K^+ channels. Implications for the study of the I(to2) current. *Circ. Res.*, **81**, 711–718 (1997).
12) Malykhina AP, Shoeb F, Akbarali HI. Fenamate-induced enhancement of heterologously expressed HERG currents in *Xenopus* oocytes. *Eur. J. Pharmacol.*, **452**, 269–277 (2002).
13) Peretz A, Degani N, Nachman R, Uziyel Y, Gibor G, Shabat D, Attali B. Meclofenamic acid and diclofenac, novel templates of KCNQ2/Q3 potassium channel openers, depress cortical neuron activity and exhibit anticonvulsant properties. *Mol. Pharmacol.*, **67**, 1053–1066 (2005).
14) Fernandez D, Sargent J, Sachse FB, Sanguinetti MC. Structural basis for ether-a-go-go-related gene K^+ channel subtype-dependent activation by niflumic acid. *Mol. Pharmacol.*, **73**, 1159–1167 (2008).
15) Zwart R, Oortgiesen M, Vijverberg HP. Differential modulation of alpha 3 beta 2 and alpha 3 beta 4 neuronal nicotinic receptors expressed in *Xenopus* oocytes by flufenamic acid and niflumic acid. *J. Neurosci.*, **15**, 2168–2178 (1995).
16) Hu H, Tian J, Zhu Y, Wang C, Xiao R, Herz JM, Wood JD, Zhu MX. Activation of TRPA1 channels by fenamate nonsteroidal anti-inflammatory drugs. *Pflugers Arch.*, **459**, 579–592 (2010).
17) Furuta A, Rothstein JD, Martin LJ. Glutamate transporter protein subtypes are expressed differentially during rat CNS development. *J. Neurosci.*, **17**, 8363–8375 (1997).
18) Poulsen MV, Vandenberg RJ. Niflumic acid modulates uncoupled substrate-gated conductances in the human glutamate transporter EAAT4. *J. Physiol.*, **534**, 159–167 (2001).
19) Arriza JL, Fairman WA, Wadiche JI, Murdoch GH, Kavanaugh MP, Amara SG. Functional comparisons of three glutamate transporter subtypes cloned from human motor cortex. *J. Neurosci.*, **14**, 5559–5569 (1994).
20) Chaudhry FA, Lehre KP, van Lookeren Campagne M, Ottersen OP, Danbolt NC, Storm-Mathisen J. Glutamate transporters in glial plasma membranes: highly differentiated localizations revealed by quantitative ultrastructural immunocytochemistry. *Neuron*, **15**, 711–720 (1995).
21) Takahashi K, Ishii-Nozawa R, Takeuchi K, Nakazawa K, Sato K. Two non-steroidal anti-inflammatory drugs, niflumic acid and diclofenac, inhibit the human glutamate transporter EAAT1 through different mechanisms. *J. Pharmacol. Sci.*, **112**, 113–117 (2010).
22) DeCoursey TE, Cherny VV. Voltage-activated hydrogen ion currents. *J. Membr. Biol.*, **141**, 203–223 (1994).
23) Fairman WA, Sonders MS, Murdoch GH, Amara SG. Arachidonic acid elicits a substrate-gated proton current associated with the glutamate transporter EAAT4. *Nat. Neurosci.*, **1**, 105–113 (1998).
24) Vandenberg RJ, Huang S, Ryan RM. Slips, leaks and channels in glutamate transporters. *Channels* (Austin), **2**, 51–58 (2008).
25) Sato K, Matsuki N, Ohno Y, Nakazawa K. Estrogens inhibit L-glutamate uptake activity of astrocytes *via* membrane estrogen receptor alpha. *J. Neurochem.*, **86**, 1498–1505 (2003).
26) Nowak L, Ascher P, Berwald-Netter Y. Ionic channels in mouse astrocytes in culture. *J. Neurosci.*, **7**, 101–109 (1987).
27) Sacher A, Cohen A, Nelson N. Properties of the mammalian and yeast metal-ion transporters DCT1 and Smf1p expressed in *Xenopus laevis* oocytes. *J. Exp. Biol.*, **204**, 1053–1061 (2001).
28) Vandenberg RJ, Arriza JL, Amara SG, Kavanaugh MP. Constitutive ion fluxes and substrate binding domains of human glutamate transporters. *J. Biol. Chem.*, **270**, 17668–17671 (1995).
29) Wadiche JI, Amara SG, Kavanaugh MP. Ion fluxes associated with excitatory amino acid transport. *Neuron*, **15**, 721–728 (1995).
30) Deitmer JW, Rose CR. pH regulation and proton signalling by glial cells. *Prog. Neurobiol.*, **48**, 73–103 (1996).
31) Muller T, Moller T, Neuhaus J, Kettenmann H. Electrical coupling among Bergmann glial cells and its modulation by glutamate receptor activation. *Glia*, **17**, 274–284 (1996).

The Journal of Toxicological Sciences (J. Toxicol. Sci.)
Vol.38, No.3, ***-***, 2013

Toxicomics Report

Comparative gene expression analysis of the amygdala in autistic rat models produced by pre- and post-natal exposures to valproic acid

Atsuko Oguchi-Katayama[1], Akihiko Monma[2], Yuko Sekino[1], Toru Moriguchi[2] and Kaoru Sato[1]

[1]Laboratory of Neuropharmacology, Division of Pharmacology, National Institute of Health Sciences, 1-18-1 Kamiyoga, Setagaya-ku, Tokyo 158-8501, Japan
[2]Department of Food and Life Sciences, Azabu University, 1-17-71 Fuchinobe, Tyuoku, Sagamihara-shi, Kanagawa 252-5201, Japan

(Received October 24, 2012; Accepted March 14, 2013)

ABSTRACT — Gene expression profiles in the amygdala of juvenile rats were compared between the two autistic rat models for mechanistic insights into impaired social behavior and enhanced anxiety in autism. The rats exposed to VPA by intraperitoneal administration to their dams at embryonic day (E) 12 were used as a model for autism (E2IP), and those by subcutaneous administration at postnatal day (P) 14 (P14SC) were used as a model for regressive autism; both of the models show impaired social behavior and enhanced anxiety as symptoms. Gene expression profiles in the amygdala of the rats (E12IP and P14SC) were analyzed by microarray and compared to each other. Only two genes, Neu2 and Mt2a, showed significant changes in the same direction in both of the rat models, and there were little similarities in the overall gene expression profiles between them. It was considered that gene expression changes per se in the amygdala might be an important cause for impaired social behavior and enhanced anxiety, rather than expression changes of particular genes.

Key words: Valproic acid, Amygdala, Microarray, Prenatal, Postnatal

INTRODUCTION

There are two similar but different kinds of autistic animal models produced by perinatal exposure of rodents to valproic acid (VPA). Rodents exposed to VPA on embryonic day (E) 12 have been used as an animal model for autism characterized by impaired social behavior, enhanced anxiety, and decreased sensitivity to pain after maturation (Markram *et al.*, 2008; Schneider and Przewtocki, 2005; Schneider *et al.*, 2007, 2008). On the other hand, rodents exposed to VPA on postnatal day (P) 14 have been used as an animal model for regressive autism that shows impaired social behavior like animal models for autism but accompanied by loss of some acquired skills (Yochum *et al.*, 2008, 2010; Wagner *et al.*, 2006). The regressive autism model also showed enhanced anxiety in our preliminary study.

The amygdala has been considered critical for behaviors associated with emotional disorders. Possible mechanisms of impaired social behavior in autism involve neural networks including the amygdala (Neuhaus *et al.*, 2010). The amygdala has also been identified to be involved in anxiety behaviors (Blackford and Pine, 2012). In humans, the amygdala and prefrontal cortex is the responsible for anxiety disorders (Etkin and Wager, 2007). It is therefore expected that comparative analysis of the amygdala in the two animal models for autism provide some mechanistic insights into impaired social behavior and enhanced anxiety in autism from similarities between them.

In the present study, we performed comparative gene expression analysis of the amygdala and characterize the similarities between the animal models for autism and for regressive autism. We first confirmed the effect of postnatal exposure to VPA on anxiety-related behavior in rats. We then compared gene expression profiles in the amygdala of juvenile rats between prenatal and postnatal exposures to VPA.

Correspondence: Kaoru Sato (E-mail: kasato@nihs.go.jp)

MATERIALS AND METHODS

Animals and VPA treatment

Pregnant Wistar Hannover/Rcc rats were obtained from Japan SLC, Inc. (Shizuoka, Japan) and maintained individually under conventional conditions with controlled temperature (23 ± 3°C) and illumination (12 hr; 7:00-19:00). Each of five litters was culled to 10 pups/litter on day 2 after birth for matched nursing conditions. For postnatal exposure, saline or 400 mg/kg of VPA (Sigma, St. Louis, MO, USA) was administered subcutaneously (s.c.) to half of the pups in each litter on postnatal day 14 (P14SC). For prenatal exposure, saline or 600 mg/kg of VPA was administered intraperitoneally (i.p.) to five pregnant rats on E12 (E12IP). Microarray analysis was performed at 5 (E12IP and P14SC) or 7 (P14SC7w) wks after the VPA administrations (Fig. 1). All animal treatments and experimental protocols were approved by the Animal Care and Use Committee of the Azabu University and the National Institute of Health Science (NIHS), and followed the Guide for the Care and Use of Laboratory Animals.

Behavioral test for anxiety

As a behavioral test, elevated plus maze (EPM) was performed in P14SC at 5 wks old with a maze consists of two opposite open arms (50 × 10 cm) and two opposite enclosed arms. The arms are connected by a central 10-cm square, forming a plus shape. The maze was elevated 50 cm above the floor. The animal's path was observed for 5 min after a resting period of 2 min in the central square of the maze. The number of entries into the open arms and the time spent in the open arms were measured.

Microarray analysis

Microarray analysis was performed using animals different from those used for behavioral test. The amygdalae were removed from the juvenile rats, and incubated in a RNA stabilization solution (RNAlater, Ambion, Austin, TX, USA) (1 ml for 5 x 5 x 5 (mm) block) overnight. Total RNA samples from the amygdalae were isolated with TRIzol (Invitrogen, Carlsbad, CA, USA) and the RNeasy Mini Kit (Qiagen, Hilden, Germany), with slight modifications to the manufacturer's protocol. The

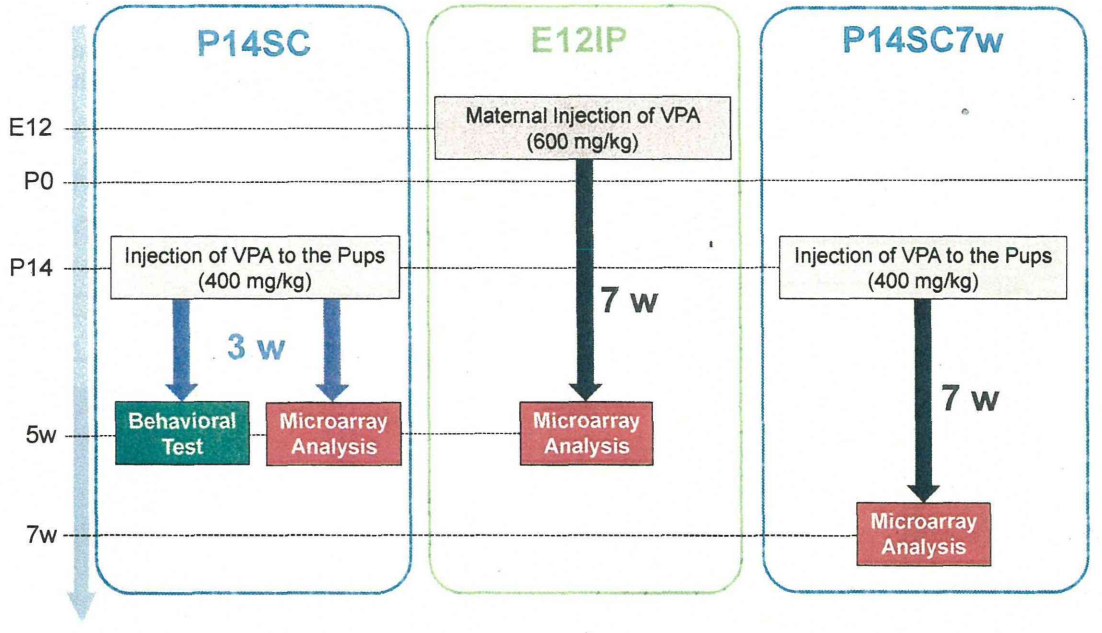

Fig. 1. The experimental design. To investigate the effect of postnatal VPA exposure on behavior and gene expression profiles, saline or 400 mg/kg VPA was administered to half of the pups per one litter subcutaneously on postnatal day 14 (P14SC). Behavior test and microarray analysis were performed using individual animals. To avoid influence of the dams, 5w juvenile rats (P35-37) were obtained evenly from 5 litters for control group and VPA- treated group, respectively. To investigate the effect of prenatal exposure, five pregnant rats were treated intraperitoneally (i.p.) with saline or 600 mg/kg VPA on E12.5 (E12IP), respectively, and microarray analysis was performed at 5w (P35-37). To analyze the contribution of the length of time from VPA exposure to cRNA isolation to the change in gene expression profile, microarray analysis was also performed at 7w (P49-56) (5 w after VPA exposure at P14) (P14SC7w).

isolated RNA sample (100 μg) were used for the microarray analysis (Affymetrix GeneChip Rat Genome 230 2.0 array (Santa Clara, CA, USA)) according to the Affymetrix protocol (http://www.affymetrix.com/support/technical/manuals.affx). Data were collected using Affymetrix GeneChip® Operating Software (GCOS) (http://media.affymetrix.com/support/technical/whitepapers/sadd_whitepaper.pdf).

Data analysis

Data analyses were carried out with GeneSpring (Agilent Technologies, Santa Clara, CA, USA). All of the data from the VPA-treated groups were normalized to the median of the control groups, and the expression of each selected gene was calculated as a log ratio of the signal to the control value. To assess the differences between the control and VPA-treated groups, the Benjamini and Hochberg false-discovery rate (FDR) method was employed, and those with a p-value less than 0.05 were considered as significant. Network, function, and pathway analyses were performed using Ingenuity Pathway Analysis software (IPA; Ingenuity Systems, Redwood City, CA, USA).

RESULTS AND DISCUSSION

Behavioral tests for anxiety

The time spent in the open arms was significantly shorter in the males of P14SC than in those of the corresponding control, indicating enhanced anxiety by postnatal exposure to VPA (Fig. 2, left). There were, however, no significant changes in the behavior test of the females (Fig. 2, right). There were no effects of the VPA exposure on the number of entries into the open arms in both genders (data not shown). These results indicate that postnatal exposure to VPA caused enhanced anxiety specifically in males. This sexual dimorphism is a typical feature of autism and has been observed in the animal model for autism produced by prenatal exposure to VPA (Schneider *et al.*, 2008). We therefore analyzed the gene expression profile of the amygdala exposed to VPA only in males in the following experiments.

Gene expression microarray analysis

In the controls, gene expression profiles were almost identical among the varied VPA exposure conditions. The number of genes with expression levels different from those in the corresponding controls was larger in P14SC (53 probe sets for 49 genes) than in E12IP (32 probe sets for 30 genes), excluding expressed sequence tags (Fig. 3A). Functional classification of the genes also indicated the differences of gene expression between P12IP and P14SC (Fig. 3B). P14SC contained a wider variety of categories than E12IP; 'phosphatase' appeared only in E12IP, while 'cytokine', 'growth factor', 'lig-

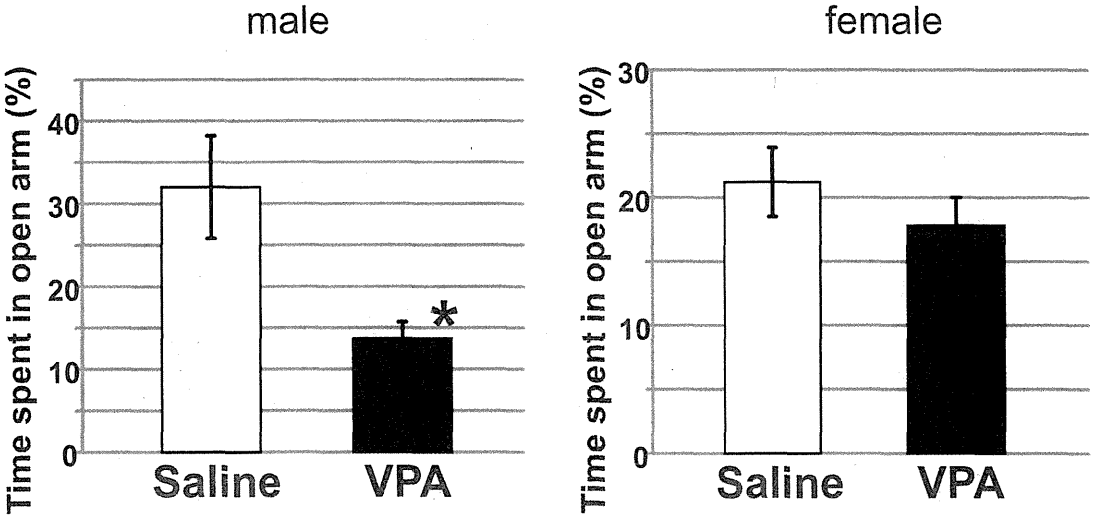

Fig. 2. The effects of postnatal exposure to VPA on anxiety-related behavior. 400 mg/kg VPA was administered to animals subcutaneously at P14. Anxiety-related behaviors were analyzed at 5w by EPM. Total open arm entries and time spent in open arm are quantified. The data of time spent in open arm were shown. An asterisk indicates a statistically significant difference from the control ($P < 0.05$, $N = 13$-15, Student's t test).